



Design and optimization of a sustainable and resilient mask supply chain during the COVID-19 pandemic: A multi-objective approach

Milad Alizadeh-Meghrazi^{1,4} · Babak Mohamadpour Tosarkani² · Saman Hassanzadeh Amin³ · Milos R Popovic¹ · Payman Ahi³

Received: 16 December 2021 / Accepted: 29 July 2022
© The Author(s), under exclusive licence to Springer Nature B.V. 2022

Abstract

Wearing a mask or a face covering became mandatory in indoor public spaces to reduce the spread of coronavirus disease 2019 (COVID-19). The Ontario government (i.e., a province of Canada) encouraged medical supply producers to switch their operations to produce personal protective equipment (e.g., masks) during the COVID-19 pandemic. In this regard, there are several uncertain parameters (e.g., operational costs, market demand, and capacity levels of facilities) affecting the performance of producers in a medical supplies market. In this study, we propose a flexible optimization model to configure a robust mask supply chain network under uncertainty. Furthermore, companies are supposed to undertake their operations based on sustainable manners, in compliance with provincial policy, in Ontario. Therefore, the proposed flexible optimization model is extended to a robust multi-objective model to investigate sustainable strategies in a mask supply chain network design problem. The applicability of this model is demonstrated for the Greater Toronto Area, Canada.

Keywords Supply chain network · Multi-objective model · Mixed-integer linear programming · Robust optimization · COVID-19 outbreak

1 Introduction

The recent COVID-19 outbreak caused major uncertainty for supply chain networks (SCNs) across the world. A general structure of SCNs may consist of multiple echelons such as suppliers, producers, distribution centers, retailers, and customer zones. A successful SCN design should have sufficient flexibility to fulfill customer expectations in

✉ Babak Mohamadpour Tosarkani
babak.tosarkani@ubc.ca

¹ Institute of Biomedical Engineering, University of Toronto, Toronto, ON, Canada

² School of Engineering, University of British Columbia, Okanagan Campus, Kelowna, BC, Canada

³ Department of Mechanical and Industrial Engineering, Toronto Metropolitan University, Toronto, ON, Canada

⁴ Myant Inc, Etobicoke, Canada

high-risk situations. The adoption of proactive strategies (e.g., inventory planning for handling fluctuations in supply and demand) leads to mitigating structural risks in uncertain circumstances (Amin & Zhang, 2013; Iyengar et al., 2020; Olivares-Aguila & ElMaraghy, 2021; Tosarkani et al., 2020). Two types of operational and disruption risks may occur in SCNs. The operational risk is caused by daily disturbance such as volatility in demand, while the disruption risk stems from high-impact events such as earthquakes, strikes, and disease outbreaks. Accordingly, the disruption risk leads to a significant impact on the structure of SCNs since some facilities may become unavailable (Govindan et al., 2020; Ivanov, 2020).

SCNs incorporate all strategic, tactical, and operational decisions (e.g., opening new facilities, partner selection, procurement, production and inventory planning, customer service, logistics, and transportations) through the collaboration between multiple entities (e.g., producers and intermediaries) to fulfill customer expectations (Yousefi et al., 2021; Rezaee et al., 2017). In supply chain planning, efforts should be implemented to coordinate materials, information, and financial flows (Choi et al., 2017; Yousefi & Tosarkani, 2022). As mentioned previously, there are several sources of uncertainties affecting SCN configuration. Hence, different mathematical approaches can be applied to deal with uncertainties in facility location problems (e.g., robust optimization, stochastic, and possibilistic programming). The adoption of such methods depends on the type of imprecise (i.e., uncertain) parameters incorporating into optimization models. Robust optimization is applicable when variations of parameters are definable (e.g., bounded uncertainty sets) (Ben-Tal & Nemirovski, 2002; Prakash et al., 2020; Vahdani & Mohammadi, 2015). Stochastic programming is employed when probability distributions of random parameters are known (Amin et al., 2017; Badri et al., 2017; Lima et al., 2018). However, in some cases, the statistical distributions of uncertain parameters (e.g., fluctuations in capacity levels of resources due to prevention policies and practices during the COVID-19 pandemic) cannot be estimated. In such cases, the fuzzy theory is applied to define imprecise parameters through a membership function (Amin et al., 2020; Tsao et al., 2018).

The World Health Organization (WHO) has declared that the coronavirus spreads primarily from person to person through small droplets from the nose or mouth when the person with COVID-19 coughs, sneezes, or speaks. Masks are supposed to be used to keep full protection of the eyes, nose, and mouth. On this matter, the presence of an efficient, effective, and robust mask SCNs is essential for COVID-19 prevention. This research is inspired by a medical device SCN in the GTA, including medical manufacturer(s), distribution center(s), retailer(s), and customers. In this respect, several uncertain factors are interfering with an optimal SCN configuration. To prevent the spread of COVID-19, many employees (except essential workers) either stay at home or work from home limiting the hours of operation. Furthermore, all employees presenting at their workplace should continue to practice physical distancing. This has a negative impact on the capacity levels of entities involved in SCNs, particularly in the healthcare sector, requiring long hours of operations due to the high-volume demand. The other uncertain parameters include market demand and major variable costs of transportation, production, and holding inventory. In this study, we develop a robust flexible multi-objective programming (RFMOP) model for a mask SCN under uncertainty in the Greater Toronto Area (GTA), Canada. The developed model enables managers to create robust SCNs for managing different types of risks. Accordingly, this model considers a variety of imprecise parameters (e.g., the capacity of producers, market demand, and infection prevention policies and practices) that affect the optimal configuration of SCNs during high-impact events.

The structure of this study is organized as follows: Sect. 2 reviews the previous studies in the field of the research. The research methodology and problem definition are provided in Sects. 3 and 4, respectively. Section 5 presents the proposed mathematical models to address the defined problem and discusses the results. The practical implications of this study are discussed for practitioners in Sect. 6. Finally, Sect. 7 describes concluding remarks and future research avenues.

2 Literature review

2.1 SCN design using stochastic programming

The relevant studies using a stochastic programming (SP) model in facility location problems are reviewed in this section. Subulan et al. (2015) designed a closed-loop supply chain network (CLSCN) for lead-acid battery production, using a scenario-based stochastic and possibilistic model considering financial and collection risks. Ameknassi et al. (2016) integrated logistics outsourcing decisions in an SCN design. They established multiple scenarios, including the uncertainty of demand, the capacity of facilities, quantity and quality of returned products, and other variable costs. Keyvanshokoo et al. (2016) developed a profit maximization model to design a CLSCN considering various scenarios for stochastic transportation costs. Soleimani et al. (2016) applied a mixed-integer linear programming (MILP) model to develop a CLSCN with stochastic demand and price. Jeihoonian et al. (2017) utilized a two-stage stochastic MILP model to configure a CLSCN for modular structured products. Binary scenarios were considered to handle uncertainty in the quality of the return stream. Fahimnia et al. (2017) created a stochastic bi-objective model for a blood SCN in a disaster situation, which focused on minimizing the total cost and delivery time. Badri et al. (2017) applied a two-stage stochastic programming (TSP) model for a value-based SCN design. Fathollahi-Fard et al. (2018) investigated the economic and social aspects of a CLSCN design using a multi-objective SPM. Heydari et al. (2018) proposed an analytical model to coordinate the order quantity and service level in a seller-buyer SCN with stochastic demand. Yu and Solvang (2018) mentioned that reverse product flow may have stochastic specifications due to the unpredictable quality of returned products and the fluctuations in pricing for remanufactured items. They applied a TSP model to design a reverse logistics network (RLN) under uncertainty.

Quddus et al. (2018) developed a two-stage chance-constrained stochastic model for a bio-fuel SCN with uncertain feedstock supply (e.g., forest residues, and municipal waste). Zahiri et al. (2018) investigated the uncertainty in blood donation through a multi-stage SP model in a blood SCN. Ghelichi et al. (2018) developed a flexible SP model to design a green biodiesel SCN under the uncertainty of fuel demand. Hamdan and Diabat (2019) considered production, inventory, and location decisions using a TSP model for a blood SCN design. Poudel et al. (2019) designed a biomass SCN with regard to uncertain feedstock supply using a TSP model. Tosarkani and Amin (2019) designed a lead-acid battery CLSCN considering the environmental compliance of involved facilities. They examined multiple scenarios for recovery rates of returned products with a given probability of occurrence. Zhang et al. (2020) investigated the quick response in a two-echelon SCN with the stochastic production capacity. They developed the two-stage two-ordering model and employed dynamic programming to obtain an optimal ordering policy. Nur et al. (2021)

proposed a novel TSP model for a biofuel SCN design incorporating related uncertain parameters such as biomass quality. Lin et al. (2020) designed a vaccine SCN, including manufacturers, distributors, and retailers (e.g., hospitals). They investigated the risks and uncertainty associated with vaccine-related adverse events and temperature damage to vaccines due to malfunctions of temperature-controlling equipment.

2.2 SCN design using fuzzy programming

In some cases, it is required to apply a fuzzy optimization model to cope with epistemic uncertainty due to the imprecise nature of input data. Dai and Zheng (2015) integrated fuzzy programming and chance-constrained programming methods to deal with uncertain disposal rates, demand, and capacity levels in a CLSCN design. Sherafati and Bashiri (2016) developed a novel fuzzy optimization method to design a CLSCN with fuzzy tactical decision variables. Amin and Baki (2017) applied a fuzzy multi-objective programming (MOP) model to deal with uncertain demand for a global CLSCN design. Dai and Li (2017) designed a multi-echelon CLSCN considering fuzzy parameters (e.g., demand, capacity levels, and prices). They proposed a bi-objective model including the total profit and waste of facilities involved in their model.

Tosarkani and Amin (2018a) introduced a fully fuzzy solution approach for a battery CLSCN. All the input parameters and decision variables were assumed to be uncertain in their created model. Yu et al. (2018) designed a dual-channel SCN for agri-product concerning information uncertainty. They employed triangular fuzzy numbers (TFNs) to deal with uncertainty. Tosarkani et al. (2020) designed a scenario-based possibilistic model for an electronic RLN design. TFNs were applied to cope with the uncertainty of demand, return, and variable costs. Tirkolaee et al. (2020) applied an integrated approach, including fuzzy decision-making and MOP, to design a reliable two-echelon SCN. Zandkarimkhani et al. (2020) proposed a bi-objective MILP model to design a perishable pharmaceutical SCN under uncertainty of demand. They developed a chance-constrained fuzzy goal programming model to solve a simultaneous facility location and vehicle routing problem. Goodarzian et al. (2021) proposed a fuzzy bi-objective MILP model to address the green medicine SCN design. They used various meta-heuristic algorithms (e.g., social engineering optimization and hybrid whale optimization) to solve this model.

2.3 SCN design using robust optimization

A robust solution approach enhances the feasibility and performance of optimization models when their infeasibility costs are considerable. Mousazadeh et al. (2015) applied a robust possibilistic programming approach to design a pharmaceutical SCN concerning epistemic uncertainty. Akbari and Karimi (2015) introduced a novel robust optimization (RO) model to design a multi-echelon SCN considering process uncertainty. Bai and Liu (2016) presented a new RO approach for an SCN configuration with regard to the variability of demand. Talaei et al. (2016) developed a robust fuzzy programming model (RFPM) to design a carbon-efficient CLSCN under the uncertainty of input parameters. Guo et al. (2016) presented an RO model to design an SCN regarding macroeconomic fluctuations. Golpîra et al. (2017) introduced a robust bi-level optimization model for a green SCN configuration to mitigate the uncertainty of demand and costs of transportation and shortage. Zokaee et al. (2017) employed an RO model to design an SCN considering the uncertainty of demand, supply, and major costs.

Alavi and Jabbarzadeh (2018) applied an RO approach for a CLSCN design to deal with the uncertainty of recycled products and market demand. Kim et al. (2018) utilized an RO method for a fashion CLSCN planning under uncertainty of market demand and RL flow. Ghahremani-Nahr et al. (2019) developed an RFPM for a multi-echelon CLSCN considering discounts on the purchase of components, shortage, and uncertain parameters (e.g., demand, return, and major costs). Yavari and Geraeli (2019) introduced an RO method to design a green CLSCN for perishable items regarding uncertain demand, quantity, and quality of returned products. Hamdan and Diabat (2020) proposed a bi-objective RO model to configure a blood SCN. The bi-objective model was applied to minimize the total cost and delivery time associated with the supply of blood during the occurrence of disasters. Sinha et al. (2020) utilized an RO approach to mitigate the impact of cost disturbance due to demand variation on the configuration of a multi-echelon apparel SCN. Arabsheybani and Arshadi Khasmeh (2021) proposed a robust bi-objective multi-product mathematical model to consider resiliency and uncertainty in SCN design. In this study, the ϵ -constraint method is employed to obtain Pareto solutions for a real case in the food industry.

2.4 SCN design considering sustainability

The economic benefits have been the primary consideration in the configuration of SCNs. However, lately, the concept of circular supply chains has appeared in operations management due to the advance of technologies and the growing level of environmental awareness (Choi et al., 2020). Govindan et al. (2016) mentioned that optimization of the social responsibility along with the environmental impact of operations should be considered in addition to the economic motivations of companies in an RLN design. In this regard, they proposed an MOP model to minimize the present value of costs, the environmental impact, and maximize the social responsibility in a medical syringe recycling program. Zhang et al. (2016) proposed an MOP model (i.e., minimizing the total cost and environmental influences, and maximizing the customer coverage) for a sustainable SCN design. Soleimani et al. (2017) developed an MOP model (i.e., maximizing the total profit and fulfilling the customer demand, and minimizing the number of missed working days because of accidents) to configure a sustainable CLSCN. Nurjanni et al. (2017) introduced a new green SCN design to minimize the total cost and carbon dioxide emissions. Van Engeland et al. (2020) mentioned that a great number of benefits are associated with the domain of waste management and facility location problems such as reducing the consumption of raw materials and diverting waste from landfills and waterways. Arampantzi and Minis (2017) applied an MOP model (i.e., emissions costs, waste generation, and community development) to design a sustainable SCN. Tosarkani and Amin (2018b) developed an MOP model (i.e., the total expected profit, green practices, on-time delivery, and quality of products and services provided by third parties) to design a sustainable electronic RL using multiple-criteria decision-making (MCDM). Rohmer et al. (2019) mentioned that the current patterns of food consumption and production make a negative impact on the environment and food security for the next generation. Accordingly, they designed a sustainable SCN in the context of the global food system.

Vafaenezhad et al. (2019) developed an MOP model (i.e., the total profit, greenhouse gas emissions, consumed energy, generated waste, travel distance of employees, and employment consistency) to design a sustainable SCN in the paper industry. Hosseini-Motlagh et al. (2019) developed a coordination mechanism to obtain the optimal pricing, sustainability levels, and corporate social responsibility in a competitive RLN. Mardan et al.

(2019) proposed a bi-objective model (i.e., the total cost and environmental emissions) to design a green CLSCN. Zarei et al. (2020) proposed a multi-objective MILP (MOMILP) model (i.e., the total profit, greenhouse gas emissions, and water consumption) to design a sustainable natural gas SCN. Rabbani et al. (2020) introduced an MOMILP model (i.e., operation costs, gasoline-related costs, uncollected waste, and the number of created jobs) to design a sustainable bioethanol SCN. Dutta et al. (2020) applied an MOP model (i.e., the total cost, environmental impact, and social responsibility) to configure a sustainable RLN in the e-commerce market. Durmaz and Bilgen (2020) introduced an MOMILP model (i.e., the total expected profit and the total distance between farms and biogas facilities) to design a sustainable biomass SCN. Fung et al. (2020) investigated the external pressure and internal motivations for companies to apply a sustainable planning strategy in a fashion SCN. They employed the institutional theory through a triple bottom line framework, including social knowledge, value systems, and governmental policies. Table 1 illustrates the research contributions of some relevant research.

3 Research methodology

This research aims to develop an RFMOP for a mask SCN under uncertainty. As indicated in Fig. 1, the overall framework of this study can be summarized in three phases:

- *Phase 1:* A mask SCN is configured in the GTA considering a realistic situation arising during the COVID-19 outbreak. In this regard, a flexible optimization model (FOM) is primarily developed to minimize the total cost of the SCN.
- *Phase 2:* As mentioned previously, environmental and social objectives should be involved to design a sustainable SCN. The model proposed in Phase 1 is extended to the MOP model. The RO approach is also employed to handle the uncertainty of the mentioned imprecise parameters. Therefore, the FOM is advanced to the RFMOP model to enable decision-makers (DMs) for managing multiple objectives under uncertainty. To the best of our knowledge, such an integrated approach is novel in SCN literature.
- *Phase 3:* The MOP model includes the total cost (z_1), CO₂ emissions (z_2), and the producer capability index (CI) (z_3). Two objectives of z_1 and z_2 consist of quantitative parameters, while z_3 contains a qualitative index associated with the capability of producers to fulfill customer expectations. Hence, a fuzzy quality function deployment (QFD) model is utilized to convert the qualitative index of CI to a quantitative parameter. Then, the non-dominated solutions of the RFMOP model are computed and discussed as managerial insights for practitioners.

4 Problem definition

According to Toronto By-Law 541–2020, wearing a mask or face covering is mandatory in indoor public spaces beginning July 7, 2020. There are 25 municipalities in the GTA with a total population of 6,417,516 (Canada statistics). In this regard, millions of people are affected by such an additional measure mandated to reduce the spread of the COVID-19. The Ontario government has begun investing in medical manufacturers to redesign their operations and expand their capacity levels to make personal protective equipment (PPE) (e.g., masks, face shields, and goggles). The COVID-19 pandemic has led to unprecedented

Table 1 Review of some studies to design and optimize facility location models under uncertainty

Authors	Network	Objective*	Sustainability	Multi-period	Multi-objective	Product	Solution approach	Real locations
Subulan et al. (2015)	CLSCN	EA			✓	Battery	SP	✓
Bai and Liu (2016)	SCN	EA		nj		Food	RO and FP	
Soleimani et al. (2016)	CLSCN	EA		A		Plastic water cane	SP	
Amin and Baki (2017)	CLSCN	EA, SA		✓	✓		FP	✓
Kim et al. (2018)	CLSCN	EA				Fashion	RO	✓
Yu et al. (2018)	SCN	EA, SA	✓		✓	Agri-product	FP	
Hamdan and Diabat (2020)	SCN	EA		✓	✓	Blood	RO	✓
Tosarkani et al. (2020)	RL	EA, GA		✓	✓	Electronic	FP and SP	✓
Hasani et al. (2021)	SCN	GA		✓	✓	Medical equipment	RO	
Goodarzi et al. (2021)	SCN	GA		✓		Medical equipment	FP	
Darmawan et al. (2021)	SCN	EA		✓			SP	
Fathollahi-Fard et al. (2021)	CLSCN	GA		✓		Tire	FP	
Arani et al. (2021)	SCN	EA, GA, SA	✓	✓	✓	Blood	RO	
Arabsheybani and Arshadi Khasmeh (2021)	SCN	EA		✓		Food	RO	
Nur et al. (2021)	SCN	EA		✓		Biofuel	SP	✓
Liu et al. (2021)	CLSCN	EA				Food	RO and FP	✓
Shahedi et al. (2022)	CLSCN	EA, GA, SA	✓	✓	✓	Automotive	SP	✓
Proposed model	SCN	EA, GA, SA	✓	✓	✓	Mask	RFMOP	✓

*Green aspect (GA), economic aspect (EA), social aspect (SA)

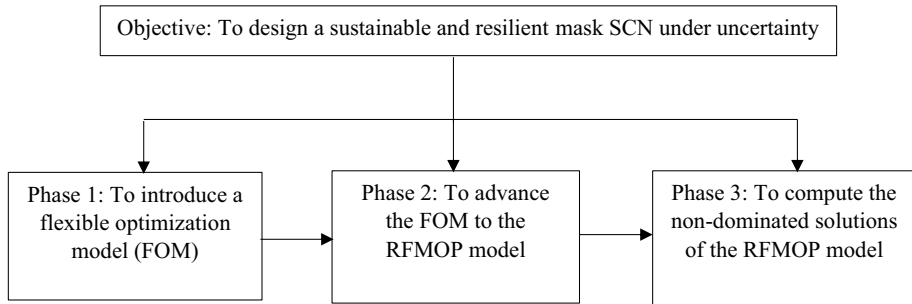


Fig. 1 The overall approach to develop a proposed RFMOP model

demand for certain PPE supplies. Accordingly, the presence of robust healthcare SCNs for the purpose of handling fluctuations in demand and different types of risks is essential.

The applicability of the proposed solution approach is investigated using a leading company in advanced manufacturing of textile technology in the healthcare industry. Their productions include textile-based wearable items (e.g., biometric clothing) for the remote monitoring of brain, heart, and muscle activities. By the beginning of the COVID-19 outbreak, they have provided textile-based PPE to reduce the spread of coronavirus disease in the GTA, Ontario.

A multi-echelon, multi-product mask SCN is illustrated in Fig. 2. The network includes producer(s), distribution center(s), retailer(s), and customer zones (markets). The producer is responsible to hold an optimal operation plan to fulfill market demand. Distribution centers are utilized for the purpose of the rapid movement of products. Retailers are located in all municipal districts. However, the number of selected retailers is mainly dependent on the fluctuations in demand during the COVID-19 outbreak. This study aims to optimize three objectives of the total cost, CO₂ emissions, and CI of the proposed SCN by answering the following questions:

- Which and how many producer(s), distribution center(s), and retailer(s) should be considered?
- How many products should be produced in each period?
- How many products should be held as the inventory and how many should be sent to the markets?

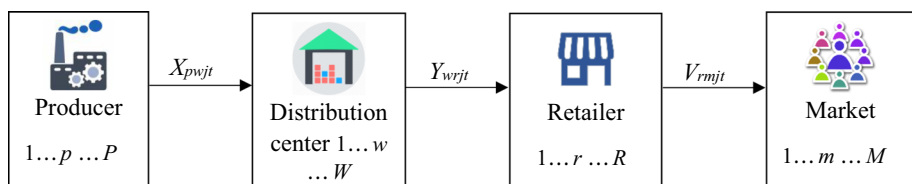


Fig. 2 The proposed mask SCN

Table 2 Indices, parameters, and decision variables used in the mathematical programming

Indices

 P : Set of potential locations for producers ($p \in P$) W : Set of distribution centers ($w \in W$) R : Set of retailers ($r \in R$) M : Set of Markets ($m \in M$) T : Set of time periods ($t \in T$) J : Set related to different types of mask supplied by producers ($j \in J$)

Parameters

 A_p : Fixed cost of agreement with producer p B_w : Fixed cost of agreement with distribution center w C_r : Fixed cost of agreement with retailer r a_j : Unit cost of transportation related to mask j between producers and distribution centers b_j : Unit cost of transportation related to mask j between distribution centers and retailers c_j : Unit cost of transportation related to mask j between retailers and markets q_{pw} : Distance between producer p and distribution center w s_{wr} : Distance between distribution center w and retailer r u_{rm} : Distance between retailer r and market m e_j : Unit cost of supply related to mask j f_j : Unit cost of holding inventory related to mask j D_{mjt} : Demand of mask j required at market m in period t E_{pj} : Capacity of producer p to produce mask j F_{wj} : Capacity of distribution center w for shipping mask j G_{rj} : Capacity of retailer r for mask j H_{pj} : Capacity of producer p for holding mask j n : Truck capacity k : Truck CO₂ emissions per km o_p : Capability of producer p to fulfill customer expectations

Decision variables

 M_{pj} : Quantity of available mask j for the supply at producer p in period t N_{pj} : Quantity of mask j holding as the inventory at producer p in period t X_{pwj} : Quantity of mask j shipping to distribution center w from producer p in period t Y_{wrj} : Quantity of mask j shipping to retailer r from distribution center w in period t V_{rmj} : Quantity of mask j shipping to market m from retailer r in period t x_p : 1, if a producer is selected at location p , 0, otherwise y_w : 1, if a distribution center is selected at location w , 0, otherwise v_r : 1, if a retailer is selected at location r , 0, otherwise

5 Flexible optimization model

An FOM is proposed to minimize the total cost of a mask SCN configuration. Table 2 indicates the notation utilized in the formulation of the FOM.

$$\begin{aligned}
 & \text{Min} z_1 \\
 & = \sum_p \sum_j \sum_t (e_j) M_{pjt} + \sum_p \sum_j \sum_t (f_j) N_{pjt} \\
 & + \sum_p \sum_w \sum_j \sum_t (a_j q_{pw}) X_{pwjt} + \sum_w \sum_r \sum_j \sum_t (b_j s_{wr}) Y_{wrjt} \\
 & + \sum_r \sum_m \sum_j \sum_t (c_j u_{rm}) V_{rmjt} + \sum_p A_p x_p + \sum_w B_w y_w \\
 & + \sum_r C_r v_r.
 \end{aligned} \tag{1}$$

Subject to the following constraints:

$$M_{pjt} + N_{pj(t-1)} - N_{pjt} = \sum_w X_{pwjt}, \quad \forall p, j, t \tag{2}$$

$$\sum_p X_{pwjt} = \sum_r Y_{wrjt}, \quad \forall w, j, t \tag{3}$$

$$\sum_w Y_{wrjt} = \sum_m V_{rmjt}, \quad \forall r, j, t \tag{4}$$

$$\sum_r V_{rmjt} \geq D_{mjt}, \quad \forall m, j, t \tag{5}$$

$$M_{pjt} \leq x_p E_{pj} + N_{pj(t-1)}, \quad \forall p, j, t \tag{6}$$

$$N_{pjt} \leq x_p H_{pj}, \quad \forall p, j, t \tag{7}$$

$$\sum_r Y_{wrjt} \leq y_w F_{wj}, \quad \forall w, j, t \tag{8}$$

$$\sum_m V_{rmjt} \leq v_r G_{rj}, \quad \forall r, j, t \tag{9}$$

$$x_p, y_w, v_r \in \{0, 1\}, \quad \forall p, w, r \tag{10}$$

$$M_{pjt}, N_{pjt}, X_{pwjt}, Y_{wrjt}, V_{rmjt} \geq 0, \quad \forall p, w, r, m, j, t. \tag{11}$$

The objective function (1) is introduced to minimize the total cost of the mask SCN design. In this regard, variable costs (i.e., costs of supply, inventory, and transportation) along with fixed costs of agreement associated with producer(s), distribution center(s),

and retailer(s) are taken into account. Constraint (2) implies that the quantity of products shipping to the distribution center(s) should be equal to the number of available products for the supply minus the number of products that must be held as the inventory in period t . Constraints (3) and (4) balance the flows between distribution center(s), retailer(s), and markets. Constraint (5) is utilized to ensure that the market demand is fulfilled. Constraint (6) represents the limit in the capacity of supply. In other words, as the nominal capacity of production (E_{pj}) in period t decreases, the number of inventory held in period ($t-1$) should be increased to cover the required number of the supply in period t . Constraint (7) indicates the maximum capacity for holding inventory, and also ensures that only the selected producer(s) can hold the inventory. Constraints (8) and (9) are associated with the capacities of distribution center(s), and retailer(s), respectively. Constraint Eq. (10) illustrates the binary variables. Finally, nonnegative decision variables are presented by Constraint Eq. (11).

5.1 A solution approach to solve the FOM

As mentioned previously, different policies (e.g., practice physical distancing, and a self-isolation period for the ones with symptoms of COVID-19) have been announced to prevent the spread of COVID-19. Such policies reduce the production capacity of producers. In this regard, producers should be flexible to fulfill market demand in a timely manner. In Constraint (7), we employ $\tilde{\leq}$, representing the soft version of \leq applied in flexible constraints, which enable producers to have the inventory more than a specific level due to the limited production capacity. Accordingly, the quantity of holding inventory is supposed to be less than or equal to the maximum capacity of producers for holding inventory. Based on Peidro et al. (2009), $N_{pjt} \tilde{\leq} x_p H_{pj}$ can be transformed into the crisp inequality constraint by $N_{pjt} \leq x_p (H_{pj}) + x_p ([\rho_{pj}(1 - \beta_p)])$, where β_p is the satisfaction level of such constraint (i.e., $0 \leq \beta_p \leq 1$), and ρ_{pj} implies the violation of the flexible constraint. In practice, ρ_{pj} can be either the emergency stock or the number of products purchased from other sources to fulfill market demand in case of operational disturbance. However, holding emergency stock imposes additional costs to the system. On this matter, ψ_{pj} is used as the unit cost of holding emergency stock. The proposed model can be rewritten as follows:

$$Minz_1 + \sum_p \sum_j \psi_{pj} (x_p ([\rho_{pj}(1 - \beta_p)])) \tag{12}$$

Subject to:

Constraints (2)–(6), (8)–(11),

$$N_{pjt} \leq x_p (H_{pj}) + x_p ([\rho_{pj}(1 - \beta_p)]), \forall p, j, t. \tag{13}$$

The multiplication of x_p by β_p in (12) and (13) causes a mixed-integer nonlinear programming (MINLP) model. To overcome nonlinearity, a nonnegative auxiliary variable of $\epsilon_p = \beta_p x_p$ is utilized to transform the MINLP model into the equivalent MILP model. Accordingly, Eqs. (12) and (13) are replaced by Eqs. (14) and (15), respectively. Furthermore, Eqs. (16)–(18) are employed based on a technique introduced by Pishvae and Khalaf (2016). Equation (16) enforces ϵ_p to be equal to zero if $x_p = 0$. Otherwise, ϵ_p is equal to β_p if $x_p = 1$ based on Eqs. (17) and (18).

$$\text{Min} z_1 + \sum_p \sum_j \psi_{pj}([\rho_{pj}(x_p - \varepsilon_p)]). \quad (14)$$

Subject to:

Constraints Eq. (2)–(6), (8)–(11),

$$N_{pj} \leq x_p(H_{pj}) + ([\rho_{pj}(x_p - \varepsilon_p)]) \forall p, j, t \quad (15)$$

$$\varepsilon_p \leq Mx_p \forall p \quad (16)$$

$$\varepsilon_p \geq M(x_p - 1) + \beta_p \forall p \quad (17)$$

$$\varepsilon_p \leq \beta_p \forall p. \quad (18)$$

5.2 Applicability of the proposed FOM

The proposed FOM is investigated using information related to the GTA. As stated, there are 25 municipal areas in the GTA considered as the regional markets. According to the mandatory mask or a face covering By-Law 541–2020, everyone is required to wear a mask in indoor public spaces (exempt children under the age of two and individuals with a medical condition). Therefore, the demand for masks in each region (market) is supposed to be equal to the population of such municipal areas. The population of each region is considered based on the 2016 census of Canada.

The unit cost of transportation is calculated as a function consisting of distances between selected facilities and the price of fuel. Hence, Google Maps is used to estimate the driving distances. The values of other parameters, incorporating into the proposed model, are set based on the case observed in the GTA (see Table 13 in Appendix 1).

IBM ILOG CPLEX 12.7.1 is applied to solve the FOM. In the proposed optimization problem, there are 645 constraints, 5,096 nonnegative decision variables, 37 binary variables, and 20,480 nonzero coefficients. The optimal solutions are obtained in 1,023 iterations and the CPU time required to solve the problem is 3 s. Table 3 illustrates the optimal configuration (i.e., the required number of facilities and flows of products) of the mask SCN in the GTA.

The optimal solutions demonstrate the balance between selected facilities. For instance, the number of masks sent to the distribution center 2 from the producer 5 (i.e., $X_{5\ 2jt} = 10,548,365$) is matched by the number of masks shipped from the distribution center 2 to the retailers (i.e., $Y_{2\ 2jt} + Y_{2\ 10jt} + Y_{2\ 13jt} + Y_{2\ 18jt} + Y_{2\ 21jt} + Y_{2\ 24jt} = 10,548,365$). As indicated in Fig. 3, the optimal network includes 1 producer, 3 sites for distribution centers, and 9 locations for retailers. Figure 4 shows the routes among the selected facilities.

Table 4 demonstrates the sensitivity analysis conducted on the nominal production capacity (E_{pj}) of the selected producer. As mentioned previously, the E_{pj} may decrease due to many factors during the COVID-19 pandemic. The 1st scenario indicates 30% decrease in the capacity of Producer 5 (E_{5j}), while β_5 is equal to 1. Recalling Eq. (13) (i.e., $N_{pj} \leq x_p(H_{pj}) + x_p([\rho_{pj}(1 - \beta_p)])$), it means that Producer 5 is still capable to handle market demand without using its emergency stock (ρ_{5j}).

Table 3 Solution for the proposed mask SCN in the GTA

Objective value ($\beta_j = 1$)	Selected producer	Selected distribution centers	Selected retailers
191,394,521	x_5 : Etobicoke	y_2 : Mississauga y_3 : Brampton y_6 : Concord	v_2 : Mississauga v_3 : Brampton v_7 : Milton v_{10} : Toronto v_{12} : Vaughan v_{13} : Markham v_{18} : Toronto v_{21} : Pickering v_{24} : Uxbridge
For all $j=1$ to 3;	$t=1$ to 2.	$M_{5 \ j} = 12,821,414$, $X_5 \ 2j = 10,548,365$, $X_5 \ 3j = 1,661,195$, $X_5 \ 6j = 611,854$, $Y_2 \ 2j = 2,195,293$, $Y_2 \ 10j = 1,245,769$, $Y_2 \ 13j = 1,556,248$, $Y_2 \ 18j = 4,500,000$, $Y_2 \ 21j = 965,555$, $Y_2 \ 24j = 85,500$, $Y_3 \ 3j = 1,441,159$, $Y_3 \ 7j = 220,036$, $Y_6 \ 12j = 611,854$, $V_2 \ 2j = 1,441,755$, $V_2 \ 5j = 387,276$, $V_2 \ 6j = 366,261$, $V_3 \ 3j = 1,186,089$, $V_3 \ 4j = 132,871$, $V_3 \ 8j = 122,200$, $V_7 \ 7j = 220,036$, $V_{10} \ 1j = 982,166$, $V_{10} \ 10j = 239,115$, $V_{10} \ 18j = 24,487$, $V_{12} \ 12j = 611,854$, $V_{13} \ 13j = 657,274$, $V_{13} \ 14j = 389,654$, $V_{13} \ 15j = 91,582$, $V_{13} \ 16j = 110,779$, $V_{13} \ 17j = 168,280$, $V_{13} \ 19j = 47,934$, $V_{13} \ 20j = 90,745$, $V_{18} \ 1j = 4,475,513$, $V_{18} \ 18j = 24,487$, $V_{21} \ 9j = 183,358$, $V_{21} \ 11j = 318,597$, $V_{21} \ 21j = 23,261$, $V_{21} \ 25j = 183,842$, $V_{24} \ 23j = 43,191$, $V_{24} \ 24j = 42,310$	

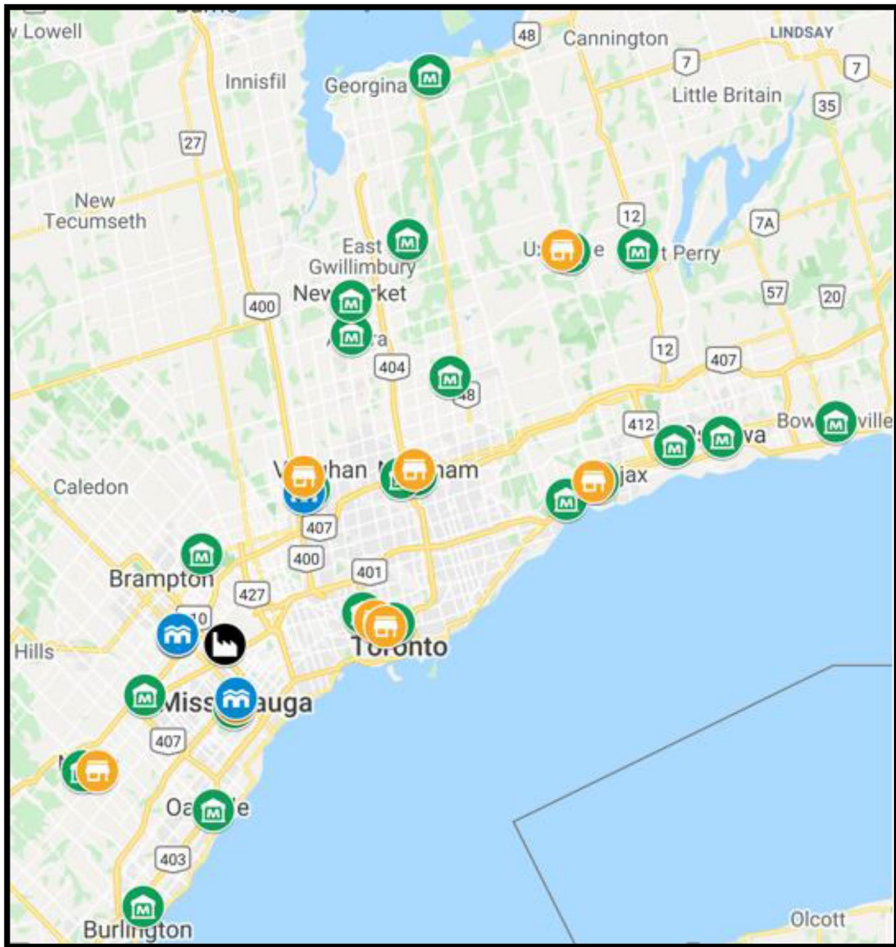


Fig. 3 The optimal mask SCN design in the GTA

However, as E_{5j} decreases by 35%, β_5 decreases from 1 to 0.72, which means that Producer 5 is not able to fulfill the market demand. Therefore, β_5 is reduced to boost the emergency stock in the selected producer (i.e., $x_5([\rho_{5j}(1 - \beta_5)])$). The 5th scenario indicates that the production capacity decreases to 50% of its nominal value. In this case, Producer 5 is not able to handle the market demand even if it uses its emergency stock; therefore, Producer 3 is added to the SCN structure.

Figure 5 illustrates the impact of the decrease in E_{5j} on the supply (M_{pj2}) in period 2 and inventory (N_{pj1}) in period 1. As a result of the decrease in E_{5j} in period 2, M_{pj2} decreases as well. Therefore, the number of N_{pj1} held in period 1 increases to fulfill customer demand (6,410,706) in period 2.

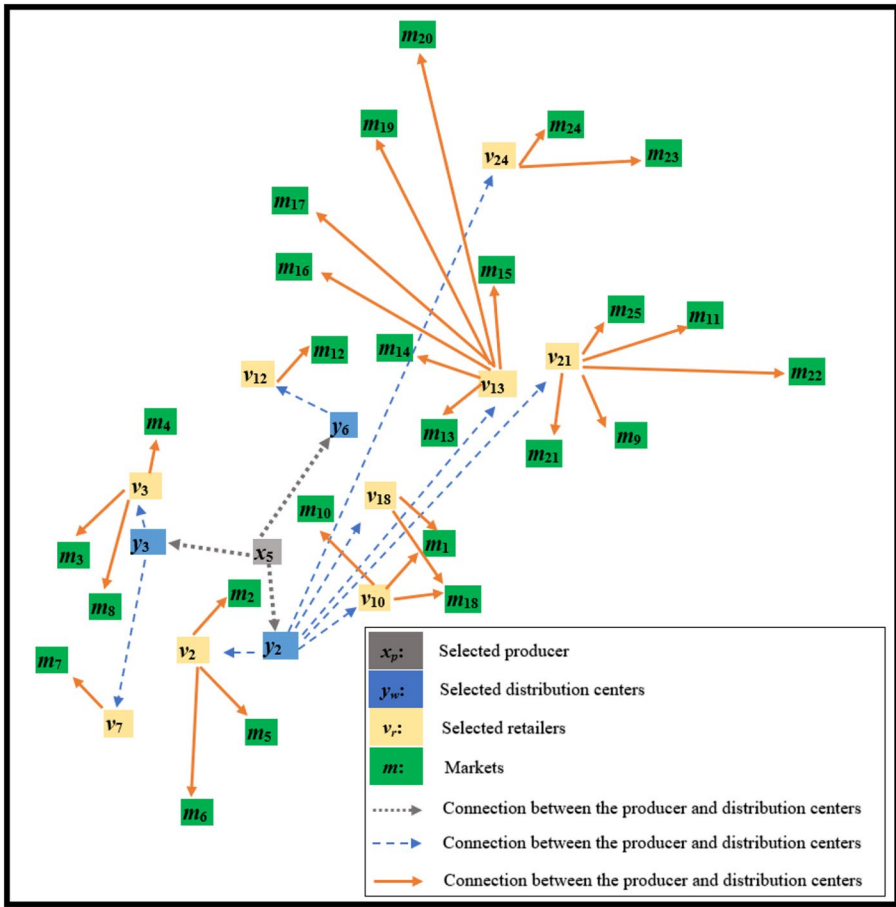


Fig. 4 The optimal routes among the selected facilities

Table 4 Sensitivity analysis of production capacity

1st scenario 30% decrease in E_{5_j}	2nd scenario 35% decrease in E_{5_j}	3rd scenario 40% decrease in E_{5_j}	4th scenario 45% decrease in E_{5_j}	5th scenario 50% decrease in E_{5_j}
196,617,701	204,180,072	212,430,072	220,680,072	290,273,898
$\beta_5 = 1$	$\beta_5 = 0.72$	$\beta_5 = 0.40$	$\beta_5 = 0.09$	$\beta_3 = \beta_5 = 1$

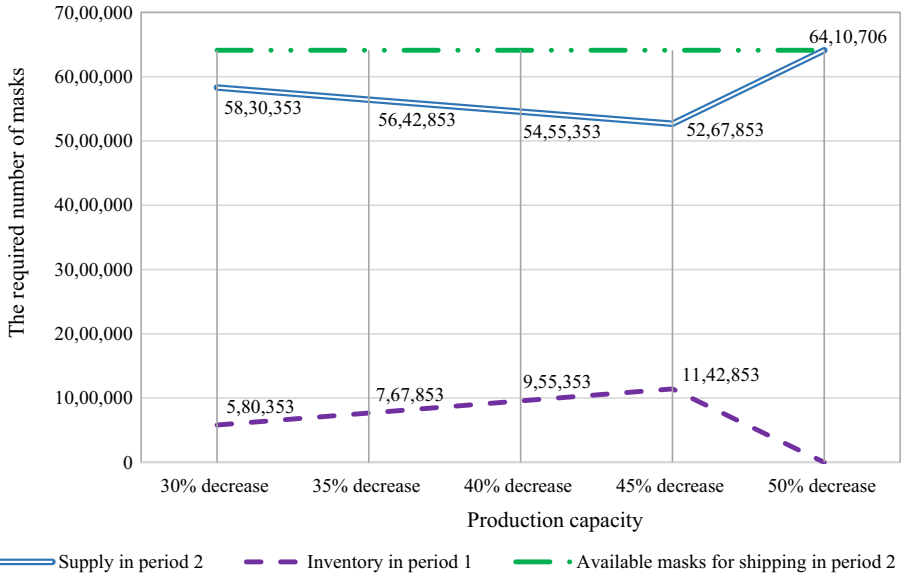


Fig. 5 The impact of operational risks on supply and inventory

5.3 An extension to an MOP model

Three aspects of economic, environmental, and social should be considered for a sustainable SCN design. The 1st objective function was introduced to investigate the economic aspect (i.e., the total cost) of the proposed model. In this section, we define Eqs. (19) and (20) to address the environmental, and social aspects of this facility location problem, respectively. Equation (19) identifies the CO₂ emissions stemming from transportation between facilities in the SCN. Furthermore, a capability index (CI) of potential producers to fulfill customer expectations is described by Eq. (20).

$$\begin{aligned}
 &Minz_2 \\
 &= k \left(\begin{aligned} &\sum_p \sum_m \sum_j \sum_t \left(\frac{X_{pwjt}}{n} \right) q_{pw} + \sum_w \sum_r \sum_j \sum_t \left(\frac{Y_{wrjt}}{n} \right) s_{wr} \\ &+ \sum_r \sum_m \sum_j \sum_t \left(\frac{V_{rmjt}}{n} \right) u_{rm} \end{aligned} \right) \tag{19}
 \end{aligned}$$

$$\begin{aligned}
 &Maxz_3 \\
 &= \sum_p \sum_w \sum_j \sum_t (o_p) X_{pwjt}. \tag{20}
 \end{aligned}$$

The CI (i.e., z_3) is a qualitative objective required to be measured by expert judgments. A fuzzy QFD model is employed to estimate the CI associated with each potential producer. The QFD process has some privileges compared to other MCDM methods since it provides a systematic approach for producers to enhance customer satisfaction. This technique is utilized in decision analysis, particularly for introducing new products. Many researchers

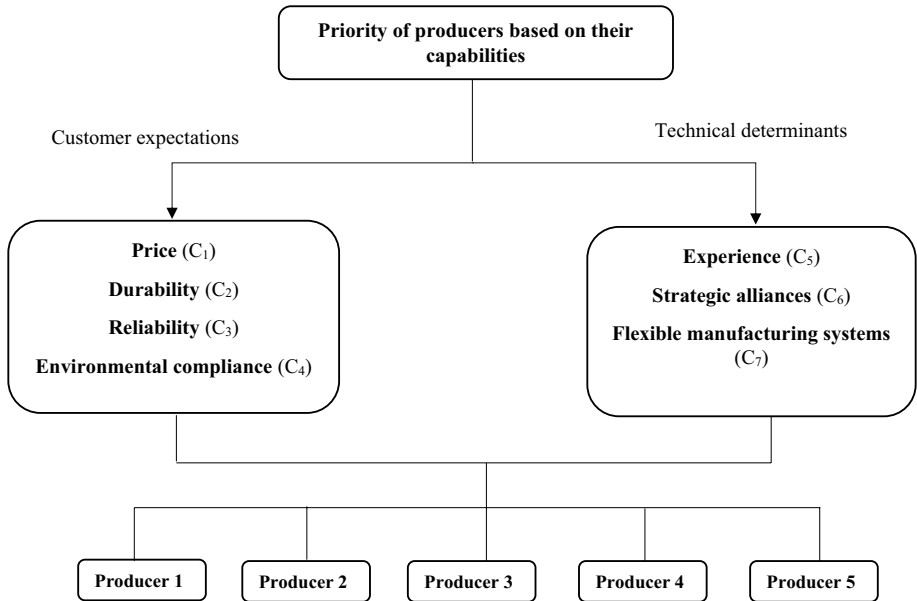


Fig. 6 An overall qualitative framework to rank the potential producers based on their capability to fulfill customer expectations

have employed QFD in different industries, such as product design process (Bottani, 2009; Karsak et al., 2003; Lee et al., 2010; Sousa-Zomer & Miguel, 2017; Zaim et al., 2014), information system development (Han et al., 1998), healthcare system (González et al., 2006), energy security management (Shin et al., 2013), employee turnover risks (Wang et al., 2014), vendor assessment and supplier recommendation for business-intelligence systems (Wang, 2015), process performance measurement system (Wieland et al., 2015), project management (Lo et al., 2017), strategic maintenance technique selection (Baidya et al., 2018), transportation sector (Chin et al., 2019; Pakdil & Kurtulmuşoğlu, 2014), and technology development (Gündoğdu & Kahraman, 2020; Haktanır & Kahraman, 2019). In QFD models, DMs play prominent roles to identify the appropriate criteria related to customer expectations and producers' technical determinants. To compare the potential producers, it is difficult to make a decision based on certain factors. Therefore, fuzzy linguistic scales can be utilized with QFD to aggregate experts' judgment in uncertain situations.

Chardine-Baumann and Botta-Genoulaz (2014) identified some major areas (e.g., customer issues, societal commitment, and business practices) to consider the social development in the configuration of sustainable SCNs. As indicated in Fig. 6, we consider price and durability, reliability of producers, and environmental compliance as indicators of customer issues, societal commitment, and business practices, respectively. Accordingly, experience, strategic alliances, and flexible manufacturing systems are considered as producers' technical determinants to fulfill customer expectations. The procedure of producer ranking is provided in Appendix 2.

5.4 An introduction of an RFMOP model

A sustainable SCN design is a strategic decision since opening or closing a facility imposes considerable costs and time. Therefore, an SCN configuration should be robust to deal with uncertain parameters (e.g., customer demand, transportation costs). Accordingly, we propose a novel RFMOP model to find the best solution that can be immunized for all possible scenarios in a specified bounded box. Model Eq. (M1) is considered to define the solution approach (Ben-Tal & Nemirovski, 2000; Ben-Tal et al., 2005; Pishvaei et al., 2011).

$$\begin{aligned}
 & \text{Min}z_1 \\
 & \text{Min}z_2 \\
 & \text{Max}z_3 \\
 & \text{s.t.} \\
 & \overset{\prime}{A}x \geq \overset{\prime}{b}, \\
 & \overset{\prime}{B}x \leq \overset{\prime}{E}\overset{\prime}{y}, \\
 & \overset{\prime}{y} \in \{0, 1\}, x \in R^+.
 \end{aligned} \tag{M1}$$

In Model (M1), $z_1 = \overset{\prime}{c}x + \overset{\prime}{d}y$ in which vector $\overset{\prime}{c}$ and $\overset{\prime}{d}$ represents variable costs and fixed costs, respectively. $\overset{\prime}{b}$ implies the market demand and $\overset{\prime}{A}$, $\overset{\prime}{B}$, $\overset{\prime}{E}$ are coefficient matrices in constraints. All variables are indicated by vectors $\overset{\prime}{y}$ (i.e., binary variables) and $\overset{\prime}{x}$ (i.e., nonnegative decision variables). In this model, all parameters of variable costs $\overset{\prime}{c}$ and market demand $\left(\overset{\prime}{b}\right)$ are presumed to be uncertain and vary in specified bounded boxes. Equation (21) shows the typical form of such boxes.

$$u_{box} = \{\gamma \in R^n : |\gamma_t - \bar{\gamma}_t| \leq \varphi\theta_t, t = 1, \dots, n\}, \tag{21}$$

where $\bar{\gamma}_t$ is the nominal value of the γ_t . θ_t is the uncertainty scale, and $\varphi > 0$ defines the uncertainty level. In this regard, a specific case of interest is $\theta_t = \bar{\gamma}_t$, therefore γ_t deviates from the nominal value to the maximum amount of φ . Furthermore, Model (M1) includes multiple objectives. The concept of the ε -constraint method is integrated to handle multiple objectives. In the ε -constraint method, the objective with the highest priority is optimized as the main objective function and the remaining objectives are considered as constraints using the ε values as the bound (Collette & Siarry, 2004; Nayak & Ojha, 2019; Roni et al., 2017). Accordingly, Model (M1) can be replaced by Model (M2).

$$\begin{aligned}
 & \text{Min} Z \\
 & \text{s.t.} \\
 & \quad \overset{\prime}{c}x + \overset{\prime}{d}y \leq Z, \forall \overset{\prime}{c} \in u_{\text{box}}^c, \\
 & \quad \overset{\prime}{A}x \geq \overset{\prime}{b}, \forall \overset{\prime}{b} \in u_{\text{box}}^b, \\
 & \quad \overset{\prime}{B}x \leq \overset{\prime}{E}y, \\
 & \quad z_2 \leq \varepsilon_2, \\
 & \quad z_3 \geq \varepsilon_3, \\
 & \quad \overset{\prime}{y} \in \{0, 1\}, x \in R^+.
 \end{aligned} \tag{M2}$$

If the bounded box is replaced by a finite set (i.e., extreme points of u_{box}), Model (M2) can be transformed into the equivalent tractable version (Ben-Tal et al., 2005; Pishvae et al., 2011). Equations (22) and (23) are the equivalent tractable versions of the constraints including uncertain parameters $\overset{\prime}{c}$ and $\overset{\prime}{b}$ varying in bounded uncertainty sets.

$$\overset{\prime}{c}x \leq Z - \overset{\prime}{d}y, \forall \overset{\prime}{c} \in u_{\text{box}}^c \left| u_{\text{box}}^c = \left\{ \overset{\prime}{c} \in R^{n_c} : \left| \frac{\overset{\prime}{c}_t - \bar{\overset{\prime}{c}}_t}{\bar{\overset{\prime}{c}}_t} \right| \leq \varphi_c \theta_t^c, t = 1, \dots, n_c \right\} \right. \tag{22}$$

$$\overset{\prime}{a}_i x \geq \overset{\prime}{b}_i, \forall i \in \{1, \dots, n_b\}, \forall \overset{\prime}{b} \in u_{\text{box}}^b \left| u_{\text{box}}^b = \left\{ \overset{\prime}{b} \in R^{n_b} : \left| \frac{\overset{\prime}{b}_i - \bar{\overset{\prime}{b}}_i}{\bar{\overset{\prime}{b}}_i} \right| \leq \varphi_b \theta_i^b, i = 1, \dots, n_b \right\} \right. \tag{23}$$

Finally, Model (M3) is written as the tractable form of Model (M2) to handle uncertain parameters as follows:

$$\begin{aligned}
 & \text{Min} Z \\
 & \text{s.t.} \\
 & \quad \sum_t \bar{\overset{\prime}{c}}_t \overset{\prime}{x}_t + \lambda_t \leq Z - \overset{\prime}{d}y, \\
 & \quad \varphi_c \theta_t^c \overset{\prime}{x}_t \leq \lambda_t, \forall t \in \{1, \dots, n_c\}, \\
 & \quad \varphi_c \theta_t^c \overset{\prime}{x}_t \geq -\lambda_t, \forall t \in \{1, \dots, n_c\}, \\
 & \quad \overset{\prime}{a}_i x \geq \bar{\overset{\prime}{b}}_i + \varphi_b \theta_i^b, \forall i \in \{1, \dots, n_b\}. \\
 & \quad \overset{\prime}{B}x \leq \overset{\prime}{E}y, z_2 \leq \varepsilon_2, z_3 \geq \varepsilon_3, \\
 & \quad \overset{\prime}{B}x \leq \overset{\prime}{E}y, \overset{\prime}{y} \in \{0, 1\}, x, \lambda \in R^+.
 \end{aligned} \tag{M3}$$

Accordingly, the robust counterpart of the mask SCN considering uncertain demand and variable costs is equivalent to the following MILP model.

$$\begin{aligned}
 & \text{Min}z_1 \\
 & = \sum_p \sum_j \sum_t \left((\bar{e}_j)M_{pjt} + \lambda_{pjt}^e \right) + \sum_p \sum_j \sum_t \left((\bar{f}_j)N_{pjt} + \lambda_{pjt}^f \right) \\
 & + \sum_p \sum_w \sum_j \sum_t \left((\bar{a}_j q_{pw})X_{pwjt} + \lambda_{pwjt}^a \right) \\
 & + \sum_w \sum_r \sum_j \sum_t \left((\bar{b}_j s_{wr})Y_{wrjt} + \lambda_{wrjt}^b \right) \tag{24} \\
 & + \sum_r \sum_m \sum_j \sum_t \left((\bar{c}_j u_{rm})V_{rmjt} + \lambda_{rmjt}^c \right) + \sum_p A_p x_p \\
 & + \sum_w B_w y_w + \sum_r C_r v_r \\
 & + \sum_p \sum_j \psi_{pj} (x_p ([\rho_{pj}(1 - \beta_p)])) .
 \end{aligned}$$

Subject to:

Constraints (2)–(4), (6), (8)–(11), (15)–(18),

$$z_2 \leq \varepsilon_2, \tag{25}$$

$$z_3 \geq \varepsilon_3, \tag{26}$$

$$\varphi_e \theta_j^e M_{pjt} \leq \lambda_{pjt}^e, \forall p, j, t \tag{27}$$

$$\varphi_e \theta_j^e M_{pjt} \geq -\lambda_{pjt}^e, \forall p, j, t \tag{28}$$

$$\varphi_f \theta_j^f N_{pjt} \leq \lambda_{pjt}^f, \forall p, j, t \tag{29}$$

$$\varphi_f \theta_j^f N_{pjt} \geq -\lambda_{pjt}^f, \forall p, j, t \tag{30}$$

$$\varphi_a \left(\theta_j^a q_{pw} \right) X_{pwjt} \leq \lambda_{pwjt}^a, \forall p, w, j, t \tag{31}$$

Table 5 Non-dominated solutions of proposed RFMOP model ($\varphi=0.15$)

Objective functions	Series 1: $\varepsilon_2=526,500$ $\varepsilon_3=1,475,000$	Series 2: $\varepsilon_2=560,500$ $\varepsilon_3=1,474,500$	Series 3: $\varepsilon_2=535,600$ $\varepsilon_3=1,625,000$	Series 4: $\varepsilon_2=619,500$ $\varepsilon_3=3,220,500$
Total cost (z_1)	315,394,216	220,433,293	315,669,473	326,882,384
CO ₂ emissions (z_2)	502,540	558,240	505,580	619,500
CI (z_3)	1,611,700	1,474,500	1,625,100	3,220,500

Table 6 Non-dominated solutions of proposed RFMOP model ($\varphi=0.30$)

Objective functions	Series 1: $\varepsilon_2=526,500$ $\varepsilon_3=1,475,000$	Series 2: $\varepsilon_2=560,500$ $\varepsilon_3=1,474,500$	Series 3: $\varepsilon_2=535,600$ $\varepsilon_3=1,625,000$	Series 4: $\varepsilon_2=619,500$ $\varepsilon_3=3,220,500$
Total cost (z_1)	544,306,199	347,113,426	444,584,884	450,698,448
CO ₂ emissions (z_2)	526,340	568,450	534,930	594,700
CI (z_3)	2,213,700	1,821,900	2,213,700	3,220,500

$$\varphi_a \left(\theta_j^a q_{pw} \right) X_{pwjt} \geq -\lambda_{pwjt}^a, \forall p, w, j, t \tag{32}$$

$$\varphi_b \left(\theta_j^b s_{wr} \right) Y_{wrjt} \leq \lambda_{wrjt}^b, \forall w, r, j, t \tag{33}$$

$$\varphi_b \left(\theta_j^b s_{wr} \right) Y_{wrjt} \geq -\lambda_{wrjt}^b, \forall w, r, j, t \tag{34}$$

$$\varphi_c \left(\theta_j^c u_{rm} \right) V_{rmjt} \leq \lambda_{rmjt}^c, \forall r, m, j, t \tag{35}$$

$$\varphi_c \left(\theta_j^c u_{rm} \right) V_{rmjt} \geq -\lambda_{rmjt}^c, \forall r, m, j, t \tag{36}$$

$$\sum_r V_{rmjt} \geq \bar{D}_{mjt} + \varphi_D \theta_{mjt}^D, \forall m, j, t \tag{37}$$

$$\lambda_{pjt}^e, \lambda_{pjt}^f, \lambda_{pwjt}^a, \lambda_{wrjt}^b, \lambda_{rmjt}^c \geq 0, \forall p, w, r, m, j, t. \tag{38}$$

5.5 Non-dominated solutions of RFMOP model considering different uncertainty levels

In MOP models, there is not a single solution that optimizes all objectives simultaneously. In such cases, several efficient solutions may exist which none of them is dominated (Deb et al., 2002; Mirzapour Al-E-Hashem et al., 2011; Tosarkani & Amin, 2018b). As demonstrated in Tables 5 and 6, we employed the RFMOP model to compute efficient solutions. In this regard, ε_2 and ε_3 are changed to reach different non-dominated solutions. By comparing Tables 5 and 6, it can be concluded that the uncertainty level (φ) has a significant impact on efficient solutions of MOP model. As demonstrated in Model (M_3), $\varphi_c \theta_j^c x_j$ is less than or equal to λ_j incorporating into the objective function. The value of φ is identified by DMs based on the type of uncertain parameters and the associated risk level.

The value path analysis (VPA) is utilized to investigate the trade-off between non-dominated solutions of RFMOP model. According to the properties of VPA, if two paths (lines) do not intersect, then an inferior line lies entirely below the superior one. In other words,

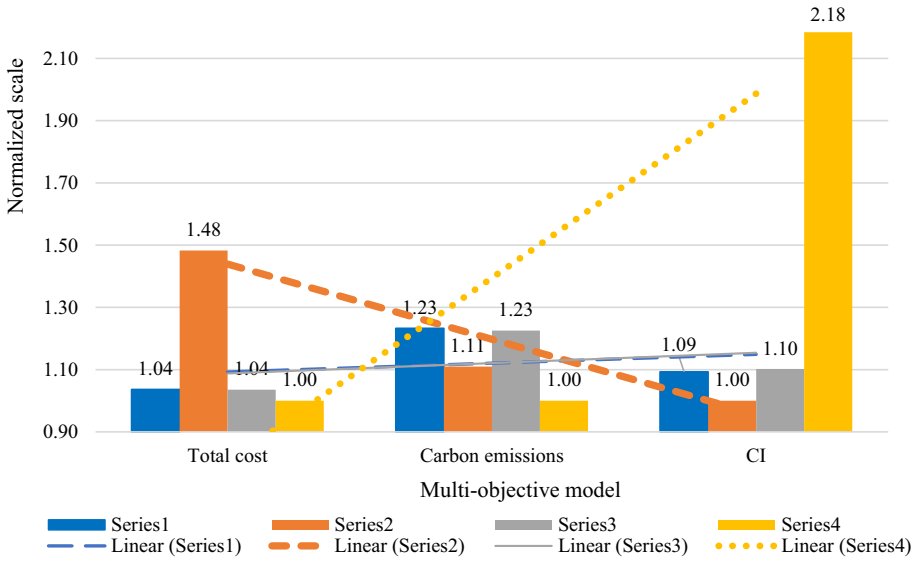


Fig. 7 Value path analysis for the non-dominated solutions of Table 5

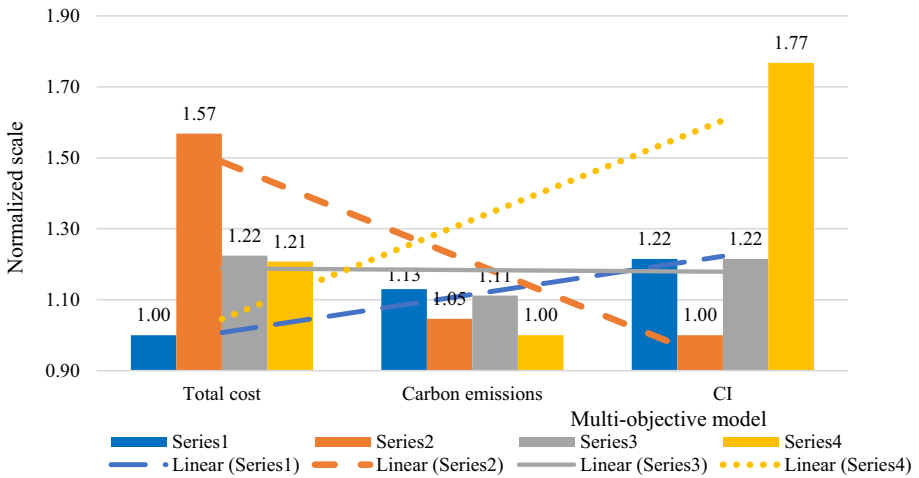


Fig. 8 Value path analysis for the non-dominated solutions of Table 6

neither of the value paths is dominated, if they have an intersection (Wadhwa and Ravindran, 2007; Afshari et al., 2020).

In the RFMOP model, we propose different types of objective functions (i.e., minimizing the total cost and CO₂ emissions along with maximizing the CI of potential producers). Therefore, the non-dominated solutions are converted to normalized measurements prior to analyzing the trade-off between them. In the case of minimization, the inferior value of one objective is divided by the corresponding values of same objective among all sets (e.g., normalized scale of z_1 : $326,882,384 / 315,394,216 = 1.04$ and z_2 : $619,500 / 502,540 = 1.23$

Table 7 Non-dominated solutions of proposed RFMOP model ($\varphi=0.15$) using distance technique

Objectives' weight	Series 1: $w_1=w_2=w_3=0.33$	Series 2: $w_1=0.8$ and $w_2=w_3=0.1$	Series 3: $w_2=0.8$ and $w_1=w_3=0.1$	Series 4: $w_3=0.8$ and $w_1=w_2=0.1$
Total cost (z_1)	316,780,000	224,130,000	419,830,000	670,230,000
CO ₂ emissions (z_2)	499,050	580,260	528,340	822,090
CI (z_3)	1,601,600	1,474,500	1,625,100	3,221,500

Table 8 Non-dominated solutions of proposed RFMOP model ($\varphi=0.30$) using distance technique

Objectives' weight	Series 1: $w_1=w_2=w_3=0.33$	Series 2: $w_1=0.8$ and $w_2=w_3=0.1$	Series 3: $w_2=0.8$ and $w_1=w_3=0.1$	Series 4: $w_3=0.8$ and $w_1=w_2=0.1$
Total cost (z_1)	364,880,000	362,020,000	547,750,000	800,970,000
CO ₂ emissions (z_2)	707,100	687,250	552,080	1,851,000
CI (z_3)	2,049,700	1,666,800	2,285,200	3,151,800

for the 1st set of Table 5). However, in the case of maximization, the objective values of a certain objective are divided by the minimum value among all alternatives (e.g., the normalized scale of z_3 : $1,611,700 / 1,474,500 = 1.09$ for the 1st set of Table 5). Accordingly, in both cases of maximizing and minimizing commands, a higher normalized scale leads to a more desirable result. Figures 7 and 8 illustrate value paths (i.e., Linear sets 1, 2, 3, and 4) for the non-dominated solutions of Tables 5 and 6, respectively. In both Figs. 7 and 8, all linear lines (Series 1, 2, 3, and 4) have intersections, and therefore, neither of them is superior based on the properties of VPA. In other words, it is verified that all the solutions are efficient.

Furthermore, the compromise programming method (i.e., a well-known method to solve the MOP model) is also considered to verify the performance of the proposed RFMOP model. This technique is utilized to compute the Pareto efficient solutions in close proximity to objectives' ideal values (Amin & Baki, 2017). Equation (39) represents the formula where w_i and z_i^* are the weight and ideal values for objective i , respectively. To compute z_i^* , each objective function is supposed to be solved separately with respect to the defined constraints (i.e., Constraints (2-4), (6), (8-11), (15-18), (25-38)). In this research, there are three objective functions including the total cost (z_1), CO₂ emissions (z_2), and CI of potential producers (z_3). Equation (40) indicated the objective function for the multi-objective mask SCN.

$$z = \left(\sum_i w_i^\tau \left(\frac{z_i - z_i^*}{z_i^*} \right)^\tau \right)^{\frac{1}{\tau}} \quad \forall i = 1, 2, \dots, \infty \tag{39}$$

Minz

$$= \left(w_1^\tau \left(\frac{z_1 - z_1^*}{z_1^*} \right)^\tau + w_2^\tau \left(\frac{z_2 - z_2^*}{z_2^*} \right)^\tau - w_3^\tau \left(\frac{z_3 - z_3^*}{z_3^*} \right)^\tau \right)^{\frac{1}{\tau}}. \tag{40}$$

Table 9 Non-dominated solutions of proposed RFMOP model ($\varphi=0.15$ and $\varepsilon_2=550,000$)

Objective functions	Series 1: $\varepsilon_2 = 550,000$ $\varepsilon_3 = 2,200,000$	Series 2: $\varepsilon_2 = 550,000$ $\varepsilon_3 = 2,300,000$	Series 3: $\varepsilon_2 = 550,000$ $\varepsilon_3 = 2,400,000$	Series 4: $\varepsilon_2 = 550,000$ $\varepsilon_3 = 2,500,000$	Series 5: $\varepsilon_2 = 550,000$ $\varepsilon_3 = 2,600,000$
Total cost (z_1)	444,584,767	444,586,627	444,885,304	445,587,759	446,568,144
CO ₂ emissions (z_2)	533,950	534,950	537,870	544,730	550,000
CI (z_3)	2,213,700	2,328,200	2,400,000	2,500,000	2,600,000

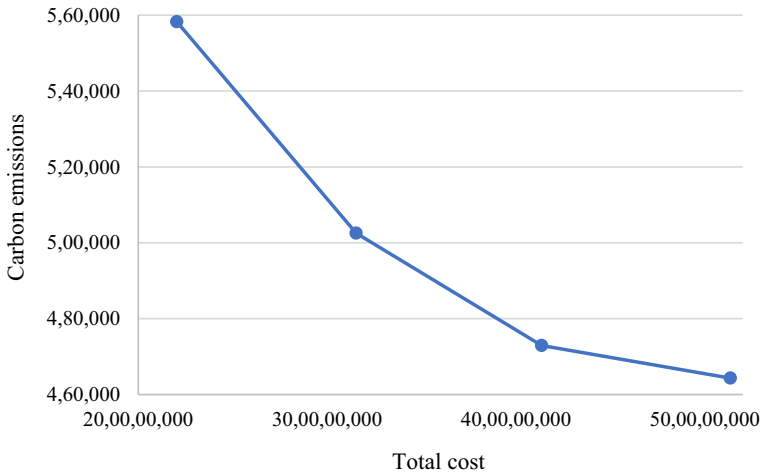


Fig. 9 The non-dominated solutions of carbon emissions and total cost

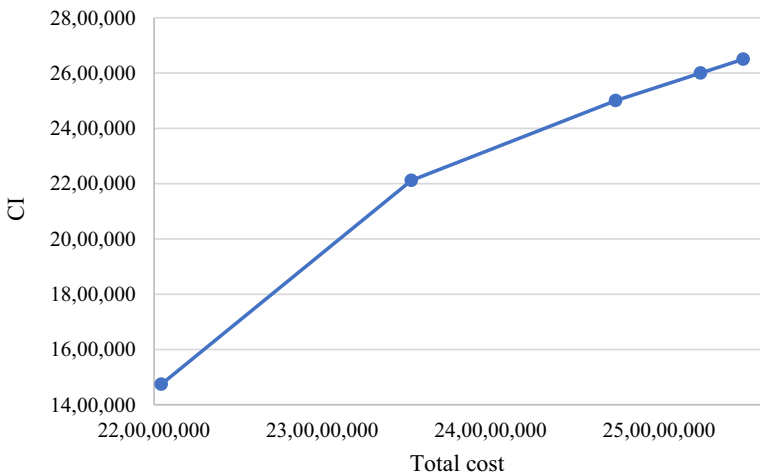


Fig. 10 The non-dominated solutions of CI and total cost

s.t.

Constraints (2)-(4), (6), (8)-(11), (15)-(18), (25)-(38).

To calculate Pareto efficient solutions of the MOP model, several pairs of w_i are tested while $\sum_i w_i = 1$. Tables 7 and 8 show the non-dominated solutions of the MOP model, while the uncertainty levels (φ) are assumed to be equal to 0.15 and 0.30.

By comparing Table 5 with Table 7 (i.e., non-dominated solutions while $\varphi=0.15$), and Table 6 with Table 8 (i.e., non-dominated solutions while $\varphi=0.30$), it can be determined that the proposed RFMOP model performs in proximity to the compromise programming method. However, the proposed RFMOP model enables DMs to compute more Pareto efficient solutions by changing ε_2 and ε_3 in desirable ranges. For example, DMs may decide

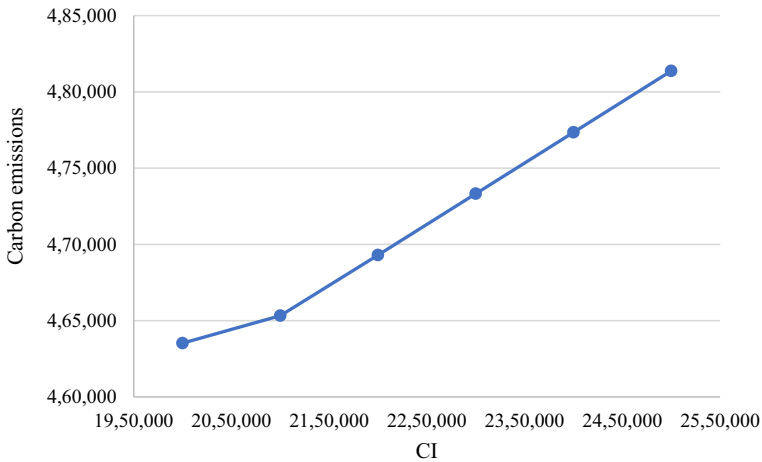


Fig. 11 The non-dominated solutions of carbon emissions and CI

to consider all non-dominated solutions in which CO_2 emissions are less than 550,000. In this case, they consider 550,000 as the value of ε_2 and change ε_3 to find different non-dominated solutions. Table 9 indicates several Pareto efficient solutions, while the CO_2 emissions are less than the specific level of 550,000.

MOP models are utilized to calculate ideal decisions in the presence of a trade-off between some conflicting objectives. As mentioned previously, a variety of Pareto efficient (i.e., non-dominated) solutions may exist for MOP problems. All non-dominated solutions are equally considered (Amin & Zhang, 2012; Deb et al., 2002). It depends on DMs to choose one of them based on their strategies. By comparing the series of non-dominated solutions in Tables 5, 6, 7, 8, and 9, it can be concluded that the value of one objective function cannot be improved without degrading the value of at least one objective function. In this study, three objectives (i.e., the total cost, carbon emissions, and CI of potential producers) are taken into account to design a sustainable mask SCN. To consider the impact of each objective on the others, three bi-objective models are solved. Figure 9 indicates that the total cost of SCN must be increased to reduce the carbon emissions stemming from transportation between facilities. Figure 10 illustrates that SCN must incur more costs to improve the CI associated with potential producers. We provide a discussion to show the reasons, as managerial insights, in Sect. 4. Similarly, as indicated in Fig. 11, the carbon emissions increase as the CI is supposed to be improved.

5.6 Application of simulation to evaluate the performance of RFMOP model

The main feature of the RFMOP model is to support strategic decisions with regard to multiple sources of uncertainty. In this section, simulation is conducted to demonstrate the performance of the proposed RFMOP model compared to the deterministic model in dealing with risks and uncertainty. Since the uncertain parameters are deviated within bounded uncertainty boxes in the proposed RFMOP model, six test problems are generated, using beta distribution, for different uncertainty levels (i.e., $\varphi = 0.15, 0.30, 0.45, 0.60, 0.75, 0.90$). The beta distribution is a continuous probability distribution, defined in terms of two parameters of α and β , on

the bounded interval (Gupta & Nadarajah, 2004; Johnson, 1997). The mean and variance of beta distribution, on the bounded interval $[v^l, v^u]$, are computed by (41) and (42).

$$\mu = v^l + (v^u - v^l) \left(\frac{\alpha}{\alpha + \beta} \right) \tag{41}$$

$$\sigma^2 = \left(\frac{\alpha}{\alpha + \beta} \right) \left(\frac{\beta}{\alpha + \beta} \right) \left(\frac{(v^u - v^l)^2}{\alpha + \beta + 1} \right) \tag{42}$$

where v^l , v^m , and v^u are the minimum, average, and maximum values of the uncertain parameter (i.e., v), respectively. The parameters of α and β can be estimated by Eqs. (43) and (44). For more information, it is recommended to refer to Davis (2008).

$$\alpha = \left(\frac{2(v^u + 4(v^m) - 5(v^l))}{3(v^u - v^l)} \right) \left(1 + 4 \left(\frac{(v^m - v^l)(v^u - v^m)}{(v^u - v^l)^2} \right) \right) \tag{43}$$

$$\beta = \left(\frac{2(5(v^u) - 4(v^m) - v^l)}{3(v^u - v^l)} \right) \left(1 + 4 \left(\frac{(v^m - v^l)(v^u - v^m)}{(v^u - v^l)^2} \right) \right). \tag{44}$$

The BETAINV (RAND (), α , β , v^l, v^u) function is employed to generate random numbers for uncertain parameters (e.g., demand and variable costs) in the bounded interval. For example, in the case of $\varphi=0.15$, v^l and v^u are considered as a 15 percent decrease and increase of v^m (i.e., nominal values of parameters). The generated random numbers (GRNs), associated with each parameter, are replicated 1,000 times. Then, the average

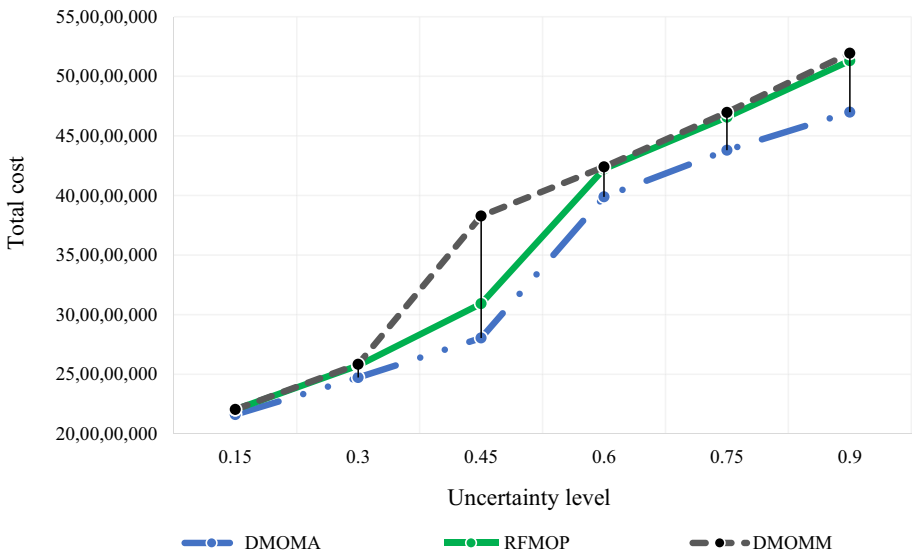


Fig. 12 Cost of robustness for RFMOP model and deterministic model

Table 10 Performances of RFMOP and DMOP models

Uncertainty level	Model	75% of capacity	50% of capacity	25% of capacity
$\varphi = 0.15$	RFMOP	x_5^*	x_3 and x_5	x_3 and x_5^*
	DMOMA	x_2 and x_5	x_3 and x_5	x_3, x_4 and x_5
	DMOMM	x_2 and x_5	x_3 and x_5	x_3, x_4 and x_5
$\varphi = 0.30$	RFMOP	x_3 and x_5	x_3 and x_5	x_3 and x_5^*
	DMOMA	x_3 and x_5	x_3 and x_5	x_3, x_4 and x_5
	DMOMM	x_3 and x_5	x_3 and x_5	x_3, x_4 and x_5
$\varphi = 0.45$	RFMOP	x_3 and x_5	x_3 and x_5	x_3 and x_5^*
	DMOMA	x_3 and x_5	x_3 and x_5	x_2, x_4 and x_5
	DMOMM	x_3 and x_5	x_3 and x_5	x_1, x_2, x_4 and x_5
$\varphi = 0.60$	RFMOP	x_3 and x_5	x_3 and x_5^*	x_3, x_4 and x_5^*
	DMOMA	x_3 and x_5	x_3, x_4 and x_5	x_1, x_3, x_4 and x_5
	DMOMM	x_3 and x_5	x_3, x_4 and x_5	x_1, x_3, x_4 and x_5
$\varphi = 0.75$	RFMOP	x_3 and x_5	x_3 and x_5^*	x_3, x_4 and x_5^*
	DMOMA	x_3 and x_5	x_3, x_4 and x_5	x_1, x_3, x_4 and x_5
	DMOMM	x_3 and x_5	x_3, x_4 and x_5	x_1, x_3, x_4 and x_5
$\varphi = 0.90$	RFMOP	x_3 and x_5	x_3 and x_5^*	x_3, x_4 and x_5^*
	DMOMA	x_3 and x_5	x_3, x_4 and x_5	x_1, x_3, x_4 and x_5
	DMOMM	x_3 and x_5	x_3, x_4 and x_5	x_2, x_3, x_4 and x_5

*The lower number of producers is required based on the RFMOP approach

and maximum values of each data set are considered to compare the performance of the RFMOP model and deterministic MOP (DMOP) model.

Constraints (25) and (26) are relaxed to indicate the impact of robustness price on the total cost of SCN precisely. To this aim, very large and small values are assigned to ε_2 and ε_3 , respectively. Then, the DMOP model is solved considering the average and maximum values of GRNs. Figure 12 demonstrates that the total cost obtained by the RFMOP model is higher than the deterministic multi-objective model solved by average values of GRNs (DMOMA) and is less than the deterministic multi-objective model solved by maximum values of GRNs (DMOMM) (i.e., worst case scenario). Therefore, the application of the RFMOP model leads to the higher total cost, compared to the DMOMA, stemming from handling risks and uncertainty (i.e., cost of robustness) in the SCN. Table 10 demonstrates the performance of the RFMOP model, DMOMA, and DMOMM in terms of the number and locations of producers (i.e., network configuration). As mentioned previously, various policies (e.g., lockdown and self-isolation period) have been considered, in Ontario, to reduce the spread of the COVID-19, which have a significant impact on the capacity levels of producers. In this regard, the RFMOP, DMOMA, and DMOMM models are solved based on different capacity levels of producers. As illustrated in Table 10, only Producers 3 and 5 (x_3 and x_5) are required to be open based on the RFMOP approach when the uncertainty level is equal to 0.15. However, the number and locations of producers are varied based on the deterministic approach (DMOMA and DMOMM) in the same level of uncertainty level. Therefore, the RFMOP model offers more stable solutions (i.e., network configuration) compared to the deterministic approach leading to the optimal utilization of producers in uncertain situations.

Table 11 Computational results of RFMOP model and DMOMM considering different uncertainty levels

Uncertainty level	100% of capacity		75% of capacity		50% of capacity		25% of capacity	
	RFMOP	DMOMM	RFMOP	DMOMM	RFMOP	DMOMM	RFMOP	DMOMM
$\varphi = 0.15$	219,728,627	219,859,291	236,237,253	315,617,187	318,680,820	319,069,511	354,494,885	425,381,455
	219,729,411	220,846,658	236,303,626	316,577,670	318,656,621	320,017,983	354,531,667	426,516,881
	219,227,661	218,285,036	235,160,378	313,909,008	318,146,940	317,399,496	353,423,667	423,330,920
	219,375,049	218,833,717	235,486,938	314,494,713	318,334,894	317,970,943	353,778,666	424,029,361
	219,751,043	219,189,072	236,306,453	314,865,798	318,679,336	318,338,947	354,537,700	424,463,291
Mean SD	219,562,358	219,402,755	235,898,930	315,092,875	318,499,722	318,559,376	354,153,317	424,744,382
	244,060	988,944	538,403	1,035,667	245,611	1,015,866	519,692	1,238,523
$\varphi = 0.30$	257,666,192	258,235,563	349,238,937	349,764,102	355,209,234	356,650,621	411,306,186	465,333,348
	257,285,375	256,463,955	348,917,012	348,243,975	354,801,878	354,857,583	410,549,274	463,348,296
	256,913,031	255,826,768	348,581,648	347,804,256	354,401,372	354,252,694	409,881,850	462,657,630
	257,415,610	257,459,379	349,026,563	349,102,363	354,935,401	355,834,276	410,771,967	464,403,203
	257,856,763	259,099,081	349,408,672	350,508,127	355,411,653	357,520,281	411,669,194	466,280,970
Mean SD	257,427,394	257,416,949	349,034,566	349,084,565	354,951,908	355,823,091	410,835,694	464,404,689
	362,719	1,317,039	316,520	1,099,363	388,411	1,319,445	691,376	1,462,106
$\varphi = 0.45$	307,231,018	378,465,134	384,377,282	382,524,297	394,824,334	394,096,264	502,423,526	504,959,981
	307,139,031	378,855,532	384,301,144	383,003,623	394,733,626	394,711,965	502,308,536	505,551,576
	307,219,825	377,375,144	384,477,057	381,289,940	394,929,542	392,437,997	502,501,283	503,334,159
	307,138,795	379,740,839	384,387,905	383,924,715	394,846,912	395,864,497	502,425,493	506,707,460
	307,076,673	380,653,108	384,200,855	384,817,526	394,678,116	397,036,957	502,304,876	507,882,961
Mean SD	307,161,068	379,017,951	384,348,849	383,112,020	394,802,506	394,829,536	502,392,743	505,687,227
	64,128	1,247,709	103,621	1,345,954	98,493	1,747,485	84,576	1,728,174

Table 11 (continued)

Uncertainty level	100% of capacity		75% of capacity		50% of capacity		25% of capacity	
	RFMOP	DMOMM	RFMOP	DMOMM	RFMOP	DMOMM	RFMOP	DMOMM
$\varphi = 0.60$	421,979,131	421,439,424	424,505,836	426,056,691	447,004,869	523,066,495	564,630,070	643,752,018
	422,046,997	421,613,651	424,567,301	426,194,271	447,171,102	523,239,028	564,798,138	643,456,454
	422,695,451	422,973,651	425,133,829	427,506,282	448,178,178	524,592,460	565,809,747	645,472,425
	421,497,773	421,151,212	424,030,779	425,787,557	446,155,114	522,779,337	563,785,446	642,855,881
	422,086,485	422,204,917	424,585,182	426,853,029	447,154,124	523,832,116	564,780,117	644,252,346
Mean SD	422,061,167	421,876,571	424,564,585	426,479,566	447,132,677	523,501,887	564,760,704	643,957,825
	426,410	724,183	391,430	695,110	718,849	720,961	719,455	985,998
$\varphi = 0.75$	466,216,778	469,303,630	468,651,408	474,072,130	512,419,398	571,079,930	630,921,956	701,774,861
	465,778,304	468,392,299	468,213,246	473,160,799	512,700,782	570,167,802	630,215,816	700,256,587
	465,013,087	467,104,035	467,454,778	471,872,535	511,205,553	568,880,138	628,776,793	698,190,720
	464,698,830	467,097,984	467,131,522	471,867,337	510,575,006	568,873,717	628,170,482	698,620,068
	465,989,598	468,874,683	468,449,166	473,643,183	512,142,965	570,650,543	630,635,639	700,324,168
Mean SD	465,539,319	468,154,526	467,980,024	472,923,197	511,808,741	569,930,426	629,744,137	699,833,281
	652,334	1,014,324	655,950	1,014,102	889,703	1,014,398	1,205,888	1,445,664
$\varphi = 0.90$	513,041,070	516,964,488	522,118,136	527,187,678	583,574,428	624,122,517	700,100,282	760,436,496
	514,189,055	519,093,563	523,467,217	529,931,205	585,476,146	626,868,283	701,994,890	763,491,934
	514,721,955	519,684,319	524,197,464	530,586,035	586,585,390	627,535,755	702,104,926	764,218,128
	513,816,525	517,882,282	523,035,155	528,415,557	584,843,067	625,295,380	701,381,542	761,823,978
	513,273,313	517,519,404	522,422,151	527,830,657	583,993,605	624,831,904	700,536,032	761,153,794
Mean SD	513,808,384	518,228,811	523,048,025	528,790,226	584,894,527	625,730,768	701,223,534	762,224,866
	680,930	1,127,847	829,685	1,427,942	1,199,403	1,426,176	884,755	1,587,823

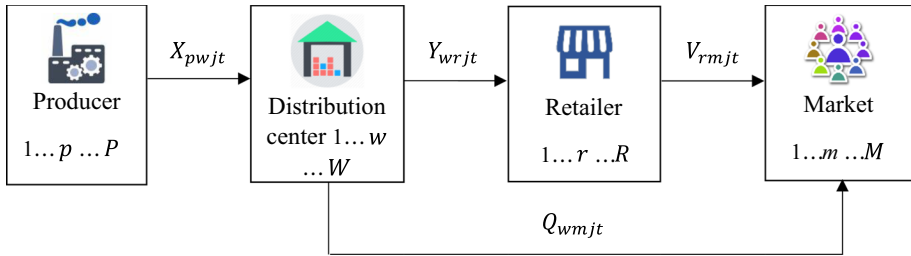


Fig. 13 The modified mask SCN considering both conventional and online purchases

Furthermore, we conduct a sensitivity analysis to evaluate the performance of the RFMOP model and DMOMM based on the mean and standard deviations of z_1 . Under different uncertainty levels, five numerical experiments, created by GRNs, are investigated with regard to different capacity levels of producers. As shown in Table 11, the RFMOP model dominates DMOMM in terms of lower standard deviations of solutions in all numerical experiments. With respect to the mean of objective functions, the results suggest that the robust flexible approach has a better performance compared to the deterministic model when the capacity of producers drops from their 100% nominal capacity levels. For further clarification, in the proposed robust flexible approach, producers are able to benefit from the emergency stock owing to the application of the flexible constraint. Therefore, as demonstrated in Table 11, the gap between the mean of the two models becomes larger as the capacity levels of producers decrease to 25% of their nominal capacity.

5.7 Incorporating online shopping into the proposed RFMOP model

As mentioned previously, this study is inspired by a textile company whose SCN is significantly affected due to the COVID-19 pandemic. This company delivers its products to the markets through distribution centers and retailers. However, online shopping has become more popular among customers to avoid COVID-19. In this section, we investigate the impact of online purchases on the network configuration. As illustrated in Fig. 13, customers may have the option to either purchase products from retailers (i.e., a conventional choice) or place online orders. In this regard, a logistics flow is required to be considered directly from distribution centers to the markets, and the proposed RFMOP model is rewritten as follows:

$$Q_{wmjt}$$

Minz₁

$$\begin{aligned}
 &= \sum_p \sum_j \sum_t \left((\bar{e}_j) M_{pjt} + \lambda_{pjt}^e \right) + \sum_p \sum_j \sum_t \left((\bar{f}_j) N_{pjt} + \lambda_{pjt}^f \right) \\
 &+ \sum_p \sum_w \sum_j \sum_t \left((\bar{a}_j q_{pw}) X_{pwjt} + \lambda_{pwjt}^a \right) + \sum_w \sum_r \sum_j \sum_t \left((\bar{b}_j s_{wr}) Y_{wrjt} + \lambda_{wrjt}^b \right) \\
 &+ \sum_r \sum_m \sum_j \sum_t \left((\bar{c}_j u_{rm}) V_{rmjt} + \lambda_{rmjt}^c \right) + \sum_p A_p x_p + \sum_w B_w y_w \\
 &+ \sum_r C_r v_r + \sum_p \sum_j \psi_{pj} (x_p ([\rho_{pj}(1 - \beta_p)])) \\
 &+ \sum_w \sum_m \sum_j \sum_t \left((\bar{g}_j i_{wm}) Q_{wmjt} + \lambda_{wmjt}^g \right)
 \end{aligned} \tag{45}$$

Minz₂

$$=k \left(\begin{aligned} &\sum_p \sum_m \sum_j \sum_t \left(\frac{X_{pwjt}}{n} \right) q_{pw} + \sum_w \sum_r \sum_j \sum_t \left(\frac{Y_{wrjt}}{n} \right) s_{wr} \\ &+ \sum_r \sum_m \sum_j \sum_t \left(\frac{V_{rmjt}}{n} \right) u_{rm} + \sum_w \sum_m \sum_j \sum_t \left(\frac{Q_{wmjt}}{n} \right) i_{wm} \end{aligned} \right). \tag{46}$$

Subject to:

Constraints (2)–(4), (6), (8)–(11), (15)–(18), (25)–(38),

$$\varphi_g \theta_j^g Q_{wmjt} \leq \lambda_{wmjt}^g, \forall w, m, j, t \tag{47}$$

$$\varphi_g \theta_j^g Q_{wmjt} \geq -\lambda_{wmjt}^g, \forall w, m, j, t \tag{48}$$

$$\sum_p X_{pwjt} = \sum_r Y_{wrjt} + \sum_m Q_{wmjt} \forall w, j, t \tag{49}$$

$$\sum_w Q_{wmjt} = \left(\bar{d}_{mjt} \right) + \varphi_D' \theta_{mjt}^D \forall m, j, t \tag{50}$$

$$\sum_r Y_{wrjt} + \sum_m Q_{wmjt} \leq y_w F_{wj} \forall w, j, t \tag{51}$$

$$Q_{wmjt}, \lambda_{wmjt}^g \geq 0, \forall w, m, j, t. \tag{52}$$

Equations (45) and (46) are applied to minimize the total cost and CO₂ emissions of the mask SCN considering both conventional and online purchases. In this regard, Q_{wmjt} denotes the number of products delivered directly from distribution center w to market m , g_j is the unit cost of transportation for mask j between distribution centers and markets, and i_{wm} refers to the distance between distribution center w and market m .

Table 12 Comparison of the network configuration in terms of conventional and online deliveries

	z_i	Objectives values	Selected producers	Selected distribution centers
1st set of Table 8 ($w_1 = w_2 = w_3 = 0.33$)	z_1	364,880,000	x_1 : Mississauga, x_5 : Etobicoke	y_1 : Toronto, y_2 : Mississauga, y_3 : Brampton, y_5 : Oakville, y_6 : Burlington
	z_2	707,100		
	z_3	2,049,700		
Considering online purchase ($w_1 = w_2 = w_3 = 0.33$) *	z_1	375,100,000	x_3 : Brampton, x_4 : Caledon	y_1 : Toronto, y_2 : Mississauga, y_3 : Brampton, y_4 : Caledon, y_5 : Oakville, y_6 : Burlington, y_7 : Milton
	z_2	822,570		
	z_3	2,078,800		

* 50% of customers place online orders

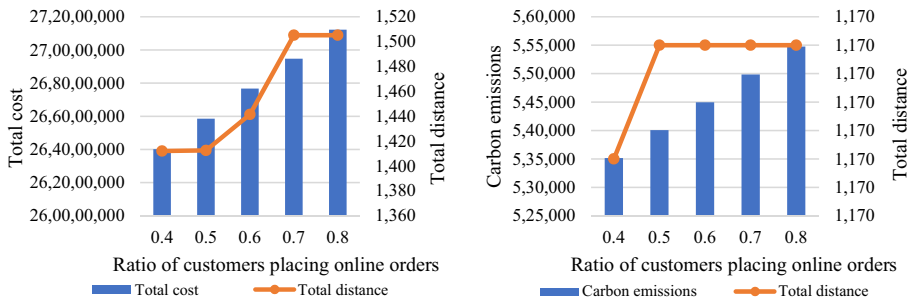


Fig. 14 Sensitivity analysis on the ratio of customers placing online orders (Note: The number of customers is fixed, therefore 0.4 implies that 40% of customers place online orders and 60% of customers purchase masks from retailers.)

Constraints (47) and (48) represent the variation of transportation costs between distribution centers and markets. Constraint (49) ensures that the quantity of products shipping to the distribution center(s) (X_{pwjt}) is equal to the number of products sending to the retailers (Y_{wrjt}) and the number of products sending to the markets (Q_{wmjt}). Constraint (50) is applied to guarantee that online orders are fulfilled. Constraint (51) is associated with the capacity of distribution center(s). Finally, Constraint (52) describes the new nonnegative variables required for direct deliveries due to online shopping.

Table 12 demonstrates the comparison between results of the 1st set of Table 8 (i.e., a conventional choice) and the modified version of the proposed RFMOP model, which considered both conventional and online purchases. As online shopping is taken into account the number of distribution centers increases to deliver the products to the customers directly. As a result, the optimal configuration of the conventional SCN changes, and the total distance between selected facilities and markets increases from 1,495 to 2,265.96 km.

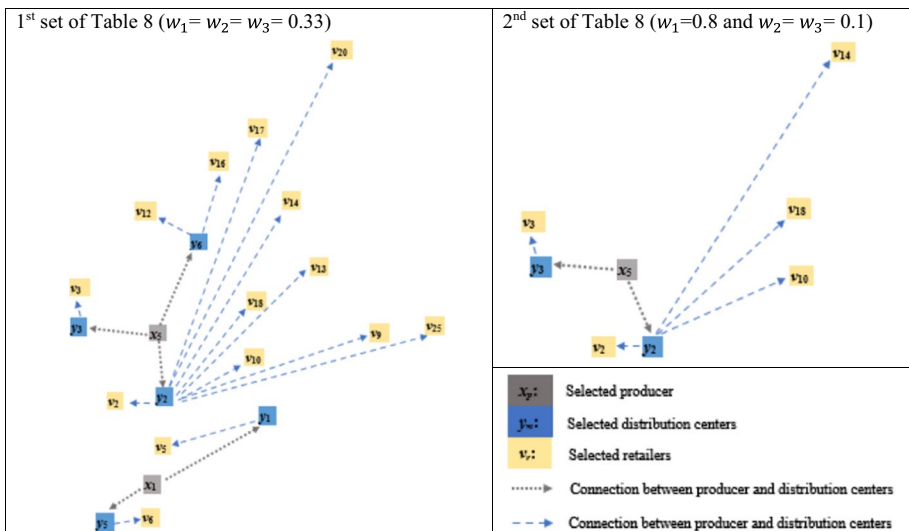


Fig. 15 Changes in SCN configuration due to the allocation of different weight to objectives by DMs

Accordingly, Table 12 indicates that the values of z_1 (i.e., total cost) and z_2 (CO₂ emissions) degrade while z_3 (i.e., CI) improves when online delivery is considered in the configuration of SCN. For further clarification, the impact of growth in online shopping is investigated on the total cost and CO₂ emissions separately. As demonstrated in Fig. 14, z_1 and z_2 increase as the ratio of customers placing online orders grows due to the increase in the total distance between selected facilities and markets.

6 Managerial insights

In a continuous outbreak, there is a variety of uncertain internal and external factors affecting the configuration of supply chains in the field of healthcare. Internal factors are concerned with the limited capacity of production and transportation, and external ones are associated with the timing and quantities of medical supply required for society. In this regard, an efficient and effective logistics capacity management can support a constant flow of production and mitigate the risk of medical device shortage during a disease outbreak.

The study of sustainable facility location models investigates the systematic determination of the number and location of facilities required to fulfill the market demand with regard to customer requirements, economic benefits, and environmental protection (Tosarkani et al., 2020; Tsai et al., 2020). In this study, the CI of producers has been optimized in addition to the total cost and CO₂ emissions for a medical SCN design. Therefore, there are several objectives which may have conflict in practice. This study attempts to offer valuable insights to managers. To this aim, let's consider the non-dominated solutions of the proposed RFMOP model provided in Table 8. We intend to compare the optimal networks for the 1st set (i.e., $w_1=w_2=w_3=0.33$) and the 2nd set (i.e., $w_1=0.8$ and $w_2=w_3=0.1$) of non-dominated solutions.

Figure 15 illustrates the comparison between the number and location of selected facilities for the two mentioned sets. As indicated in the 2nd set, 1 producer (i.e., x_5), 2 distribution centers (i.e., y_2 , and y_3), and 5 retailers (i.e., v_2 , v_3 , v_{10} , v_{14} , and v_{18}) are selected when the economic aspect has the highest priority for DMs. However, the SCN configuration is significantly different, if equal weight factors are considered for all three objectives (i.e., 1st set of Table 8). Accordingly, Producer 1, which has the highest priority in the aspect of CI (see Table 23 in Appendix 2), should operate along with Producer 5, and also the number of distribution centers and retailers increases. Therefore, the capability of producers to fulfill the customer requirements (i.e., social aspects) improves from 1,666,700 to 2,049,700. However, the total cost and CO₂ emissions of SCN are degraded from 362,020,000 to 364,880,000 and 687,250 to 707,100, respectively, since the total distance between selected facilities increases from 1057 to 1495 km. The proposed MOP model implies that at least the value of one objective must be compromised to improve the values of other objectives. This provides DMs with an opportunity to investigate the impact of each objective on the configuration of facility location models under uncertainty.

7 Conclusions

A multi-objective, multi-echelon, multi-product, multi-period model was proposed for a mask SCN in the GTA. The proposed MOP model included three objectives (i.e., the total cost, generated CO₂ emissions, CI of potential producers) to consider sustainability in a facility location problem. The proposed SCN contained multiple facilities such as producers, distribution centers, retailers, and markets. In this study, several challenges were investigated in uncertain circumstances (e.g., ongoing COVID-19 outbreak), such as matching the production capacity of producers with fluctuations in market demand. In this regard, various activities such as planning for production, inventory, and transportation were taken into account in multiple periods.

A successful SCN design should be flexible and robust to fulfill demand during high-impact events, particularly in the field of healthcare. In this study, an FOM was first introduced to utilize the emergency stock in case of a reduction in the capacity levels of producers. Another source of uncertainty was caused by imprecise input parameters (e.g., variable costs and market demand). To handle such types of uncertainty, robust optimization was integrated with the FOM to find the optimal solution that can be guaranteed by all possible scenarios. Pareto efficient (i.e., non-dominated) solutions were computed for the proposed MOP model. As demonstrated by VPA analysis, as the value of one objective function improves, the values of other objective functions degrade in the MOP model. Therefore, it depends on DMs which set of non-dominated solutions should be selected in the ongoing

Fig. 16 **A:** customer expectations (i.e., voice of customers), (WHATs) **B:** priority of customer requirements, **C:** technical determinants (i.e., voice of the organization), (HOWs), **D:** relationship matrix HOWs vs WHATs, **E:** correlation between technical determinants, **F:** priority of technical determinants

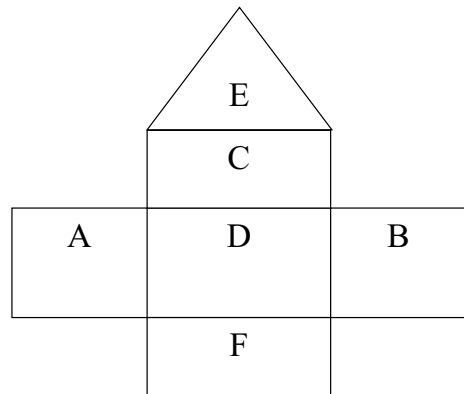


Table 13 Values of the parameters

$P=5$	$A_p=100,000,000$	$E_{pj}=(2,500,000)_{5*3}$
$W=7$	$B_w=400,000$	$H_{pj}=(500,000)_{5*3}$
$R=25$	$C_r=100,000$	$G_{rj}=(750,000)_{25*3}$
$M=25$	$e_j=4$	$F_{wj}=(3,000,000)_{7*3}$
$T=2$	$f_j=6$	$\rho_{pj}=(500,000)_{5*3}$
$J=3$	$a_j=b_j=c_j=0.107$	$n=50,000$
	$\psi_{pj}=14$	$k=68$

* o_p is calculated in Appendix 2

Table 14 Ranking of criteria

WHATs	1st DM	2nd DM	3rd DM
C ₁	VH	M	MH
C ₂	M	M	H
C ₃	H	H	H
C ₄	MH	MH	MH

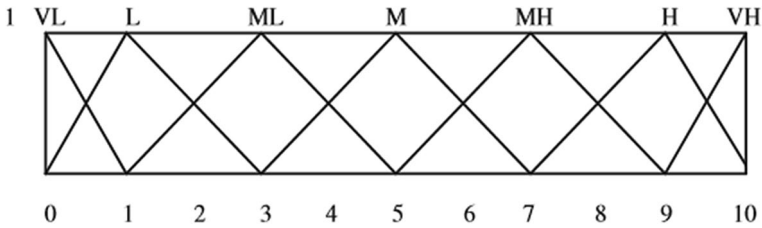


Fig. 17 Very Low (VL)=(0,0,1), Low (L)=(0,1,3), Medium Low (ML)=(1,3,5), Medium (M)=(3,5,7), Medium High (MH)=(5,7,9), High (H)=(7,9,10), Very High (VH)=(9,10,10)

Table 15 The obtained aggregated weights

WHATs	$\alpha_1 * w_{i1}$	$\alpha_2 * w_{i2}$	$\alpha_3 * w_{i3}$	Aggregated weight (w_i)
C ₁	(90, 200, 200)	(15, 50, 105)	(50, 140, 180)	(155, 390, 485)
C ₂	(30, 100, 140)	(15, 50, 105)	(70, 180, 200)	(115, 330, 445)
C ₃	(70, 180, 200)	(35, 90, 150)	(70, 180, 200)	(175, 450, 550)
C ₄	(50, 140, 180)	(25, 70, 135)	(50, 140, 180)	(125, 350, 495)

circumstance. A discussion was provided to show how the structure of an SCN might change in terms of considering different non-dominated solutions. However, it is worthy to note that an SCN configuration includes strategic decisions (e.g., third-party selection and capacity decisions), which are impossible to change in the short term. To our knowledge, this study is among the first investigations to propose an integrated RFMOP model to configure an SCN in the field of healthcare. According to our findings, the proposed RFMOP model is an effective solution approach to deal with imprecise parameters.

This research can be extended in different directions. To design a sustainable SCN, CO₂ emissions were investigated based on the driving distance. On this matter, incorporating other criteria (e.g., routing plan and traffic condition) to estimate CO₂ emissions will offer more precise results. Furthermore, various types of risks (i.e., the uncertainty of input parameters, disruptions in facilities, and transportations) may exist in real problems, and we discussed the first type of risk in this research. Therefore, it is valuable to develop the proposed model to mitigate the impact of disruptions on SCNs. In this research, the values of demand are assumed to be equal to the population of each specific region due to the mandatory face mask policy. However, demand will change after the outbreak. Therefore, developing a forecasting approach for market demand can be a future research direction for this study.

Table 16 Relationship matrix HOWs vs WHATs

HOWs WHATs	C ₅			C ₆			C ₇		
	1st DM	2nd DM	3rd DM	1st DM	2nd DM	3rd DM	1 st DM	2 nd DM	3 rd DM
C ₁	H	VH	H	H	MH	MH	VH	H	VH
C ₂	MH	M	H	ML	M	H	H	H	H
C ₃	MH	H	MH	M	H	H	MH	MH	MH
C ₄	MH	M	M	VH	VH	VH	H	H	H

Table 17 Results of relationship matrix WHATs and HOWs

HOWs WHATs (a_{ij})	C ₅	C ₆	C ₇	Aggregated weight (w_i)
C ₁	(185, 460, 550)	(145, 390, 515)	(215, 490, 550)	(155, 390, 485)
C ₂	(135, 370, 485)	(95, 290, 405)	(175, 450, 550)	(115, 330, 445)
C ₃	(135, 370, 510)	(135, 370, 490)	(125, 350, 495)	(175, 450, 550)
C ₄	(95, 290, 425)	(225, 500, 550)	(175, 450, 550)	(125, 350, 495)
f ₁ : (19,925, 142,375, 243,363)		f ₂ : (21,288, 147,325, 242,938)	f ₃ : (24,300, 163,650, 264,000)	

Table 18 The capability of producer 1 to perform technical determinants

WHATs	1st DM	2nd DM	3rd DM	Aggregated weight (PR_{1j})
C ₅	VH	VH	VH	(225, 500, 550)
C ₆	VH	VH	H	(205, 480, 550)
C ₇	H	H	VH	(195, 470, 550)

Table 19 The capability of producer 2 to perform technical determinants

WHATs	1st DM	2nd DM	3rd DM	Aggregated weight (PR_{2j})
C ₅	ML	ML	L	(15, 110, 235)
C ₆	L	ML	ML	(15, 110, 235)
C ₇	L	L	L	(0, 50, 165)

Appendix 1: Parameters

See Table 13.

Table 20 The capability of producer 3 to perform technical determinants

WHATs	1st DM	2nd DM	3rd DM	Aggregated weight (PR_{3j})
C_5	ML	ML	ML	(25, 150, 275)
C_6	L	L	L	(0, 50, 165)
C_7	L	L	L	(0, 50, 165)

Table 21 The capability of producer 4 to perform technical determinants

WHATs	1st DM	2nd DM	3rd DM	Aggregated weight (PR_{4j})
C_5	L	VL	L	(0, 40, 135)
C_6	L	L	VL	(0, 30, 125)
C_7	L	L	L	(0, 50, 165)

Table 22 The capability of producer 5 to perform technical determinants

WHATs	1st DM	2nd DM	3rd DM	Aggregated weight (PR_{5j})
C_5	VL	L	L	(0, 30, 125)
C_6	L	ML	L	(5, 70, 195)
C_7	L	L	VL	(0, 30, 125)

Table 23 Final ranking of each potential producer

Producer	FPR			Defuzzified index	Ratio	Ranking
	l	m	u			
Producer 1	4,528,521	72,939,667	137,555,000	71,674,396	50.12%	1st
Producer 2	206,063	13,349,833	52,613,500	22,056,465	15.42%	2nd
Producer 3	166,042	12,301,667	50,189,792	20,885,833	14.61%	3rd
Producer 4	0	6,099,083	35,593,708	13,897,597	9.72%	5th
Producer 5	35,479	6,497,833	36,931,042	14,488,118	10.13%	4th

Appendix 2: The QFD model

In this study, the QFD model is employed to prioritize producers based on qualitative factors. As indicated in Fig. 16, there are different sections in the QFD model (e.g., customer requirements, technical determinants).

As indicated in Fig. 6, various criteria are defined to consider both voices of customers and producers. In this study, four qualitative criteria (i.e., price, durability, reliability, and environmental compliance) are identified to represent the customer expectations and three technical criteria (i.e., experience, strategic alliances, and flexible manufacturing system) are considered to evaluate the capability of producers, respectively. Following phases are

taken into account to rank the potential producers based on their capability to fulfill customer expectations.

Phase 1: As indicated in Table 14, the following linguistic scale (i.e., Fig. 17) is utilized to rank the criteria based on the expert judgment.

Phase 2: DMs have different levels of experience that must be considered in the judgment. Therefore, it is proposed to determine the weight factors for DMs. In this study, we consider experience index (i.e., poor=(0, 0, 10), normal=(5, 10, 15), perfect=(10, 20, 20)). In this case, there are three DMs. α_n (i.e., $n=1, 2, 3$) is defined as the weight of DM_n . The 1st and 3rd DMs have the perfect level of experience, while the 2nd one has a normal level of experience. Then, (b.1) is employed to aggregate the weights assigned by DMs. The results are provided in Table 15.

$$w_i = (\alpha_1 \times w_{i1}) + (\alpha_2 \times w_{i2}) + \dots + (\alpha_N \times w_{iN}) \quad (b.1)$$

where I and N are the numbers of customer expectations and DMs, respectively.

Phase 3: As illustrated in Table 16, the linguistic scale is utilized by all three DMs to evaluate the impact of technical determinants (i.e., HOWs) on customer expectations (i.e., WHATs).

Phase 4: (b.2) and (b.3) are employed to compute the relationship matrix between customer expectations (WHATs) and technical determinants (HOWs). Table 17 indicates the results of the relationship matrix.

$$a_{ij} = (\alpha_1 \times a_{ij1}) + (\alpha_2 \times a_{ij2}) + \dots + (\alpha_N \times a_{ijN}) \quad (b.2)$$

$$f_j = \frac{1}{I} \times [(w_1 \times a_{1j}) + (w_2 \times a_{2j}) + \dots + (w_I \times a_{Ij})] \quad (b.3)$$

where a_{ij} is the aggregated weight between WHATs and HOWs. J is the number of HOWs and f_j is the weight associated with HOWs.

Phase 5: (b.4) is applied to estimate the capability (PR_{pj}) of each potential producer p to perform a technical determinant j . Tables 18, 19, 20, 21, and 22 illustrate the results.

$$PR_{pj} = (\alpha_1 \times PR_{pj1}) + (\alpha_2 \times PR_{pj2}) + \dots + (\alpha_N \times PR_{pjN}) \quad (b.4)$$

Phase 6: (b.5) is employed to calculate the final ranking of each potential producer regarding customer expectation and technical determinants. The final results are provided in Table 23.

$$FPR = \frac{1}{J} \times [(PR_{p1} \times f_1) + (PR_{p2} \times f_2) + \dots + (PR_{pJ} \times f_J)] \quad (b.5)$$

References

- Afshari, H., Tosarkani, B. M., Jaber, M. Y., & Searcy, C. (2020). The effect of environmental and social value objectives on optimal design in industrial energy symbiosis: A multi-objective approach. *Resources, Conservation and Recycling*, 158, 104825.
- Akbari, A. A., & Karimi, B. (2015). A new robust optimization approach for integrated multi-echelon, multi-product, multi-period supply chain network design under process uncertainty. *The International Journal of Advanced Manufacturing Technology*, 79(1–4), 229–244.

- Alavi, S. H., & Jabbarzadeh, A. (2018). Supply chain network design using trade credit and bank credit: A robust optimization model with real world application. *Computers and Industrial Engineering*, *125*, 69–86.
- Ameknassi, L., Ait-Kadi, D., & Rezg, N. (2016). Integration of logistics outsourcing decisions in a green supply chain design: A stochastic multi-objective multi-period multi-product programming model. *International Journal of Production Economics*, *182*, 165–184.
- Amin, S. H., & Baki, F. (2017). A facility location model for global closed-loop supply chain network design. *Applied Mathematical Modelling*, *41*, 316–330.
- Amin, S. H., & Zhang, G. (2012). An integrated model for closed-loop supply chain configuration and supplier selection: Multi-objective approach. *Expert Systems with Applications*, *39*(8), 6782–6791.
- Amin, S. H., & Zhang, G. (2013). A multi-objective facility location model for closed-loop supply chain network under uncertain demand and return. *Applied Mathematical Modelling*, *37*(6), 4165–4176.
- Amin, S. H., Zhang, G., & Akhtar, P. (2017). Effects of uncertainty on a tire closed-loop supply chain network. *Expert Systems with Applications*, *73*, 82–91.
- Amin, S. H., Zhang, G., & Eldali, M. N. (2020). A review of closed-loop supply chain models. *Journal of Data, Information and Management*, *2*(4), 279–307.
- Arabsheybani, A., & Arshadi Khasmeh, A. (2021). Robust and resilient supply chain network design considering risks in food industry: Flavour industry in Iran. *International Journal of Management Science and Engineering Management*, *16*(3), 197–208.
- Arampantzi, C., & Minis, I. (2017). A new model for designing sustainable supply chain networks and its application to a global manufacturer. *Journal of Cleaner Production*, *156*, 276–292.
- Arani, M., Chan, Y., Liu, X., & Momenitabar, M. (2021). A lateral resupply blood supply chain network design under uncertainties. *Applied Mathematical Modelling*, *93*, 165–187.
- Badri, H., Ghomi, S. F., & Hejazi, T. H. (2017). A two-stage stochastic programming approach for value-based closed-loop supply chain network design. *Transportation Research Part e: Logistics and Transportation Review*, *105*, 1–17.
- Bai, X., & Liu, Y. (2016). Robust optimization of supply chain network design in fuzzy decision system. *Journal of Intelligent Manufacturing*, *27*(6), 1131–1149.
- Baidya, R., Dey, P. K., Ghosh, S. K., & Petridis, K. (2018). Strategic maintenance technique selection using combined quality function deployment, the analytic hierarchy process and the benefit of doubt approach. *The International Journal of Advanced Manufacturing Technology*, *94*(1–4), 31–44.
- Ben-Tal, A., & Nemirovski, A. (2000). Robust solutions of linear programming problems contaminated with uncertain data. *Mathematical Programming*, *88*(3), 411–424.
- Ben-Tal, A., & Nemirovski, A. (2002). Robust optimization—methodology and applications. *Mathematical Programming*, *92*(3), 453–480.
- Ben-Tal, A., Golany, B., Nemirovski, A., & Vial, J. P. (2005). Retailer-supplier flexible commitments contracts: A robust optimization approach. *Manufacturing and Service Operations Management*, *7*(3), 248–271.
- Bottani, E. (2009). A fuzzy QFD approach to achieve agility. *International Journal of Production Economics*, *119*(2), 380–391.
- Chardine-Baumann, E., & Botta-Genoulaz, V. (2014). A framework for sustainable performance assessment of supply chain management practices. *Computers and Industrial Engineering*, *76*, 138–147.
- Chin, K. S., Yang, Q., Chan, C. Y., Tsui, K. L., & Li, Y. L. (2019). Identifying passengers' needs in cabin interiors of high-speed rails in China using quality function deployment for improving passenger satisfaction. *Transportation Research Part a: Policy and Practice*, *119*, 326–342.
- Choi, T. M., Yeung, W. K., Cheng, T. E., & Yue, X. (2017). Optimal scheduling, coordination, and the value of RFID technology in garment manufacturing supply chains. *IEEE Transactions on Engineering Management*, *65*(1), 72–84.
- Choi, T. M., Taleizadeh, A. A., & Yue, X. (2020). Game theory applications in production research in the sharing and circular economy era. *International Journal of Production Research*, *8*(1), 118–127.
- Collette, Y., & Siarry, P. (2004). Multiobjective optimization: principles and case studies. Springer Science and Business Media.
- Dai, Z., & Li, Z. (2017). Design of a dynamic closed-loop supply chain network using fuzzy bi-objective linear programming approach. *Journal of Industrial and Production Engineering*, *34*(5), 330–343.
- Dai, Z., & Zheng, X. (2015). Design of close-loop supply chain network under uncertainty using hybrid genetic algorithm: A fuzzy and chance-constrained programming model. *Computers and Industrial Engineering*, *88*, 444–457.
- Darmawan, A., Wong, H., & Thorstenson, A. (2021). Supply chain network design with coordinated inventory control. *Transportation Research Part e: Logistics and Transportation Review*, *145*, 102168.

- Davis, R. (2008). Teaching Project Simulation in Excel Using PERT-Beta Distributions. *Teaching Note. INFORMS Transactions on Education*, 8(3), 139–148.
- Deb, K., Pratap, A., Agarwal, S., & Meyarivan, T. A. M. T. (2002). A fast and elitist multiobjective genetic algorithm: NSGA-II. *IEEE Transactions on Evolutionary Computation*, 6(2), 182–197.
- Durmaz, Y. G., & Bilgen, B. (2020). Multi-objective optimization of sustainable biomass supply chain network design. *Applied Energy*, 272, 115259.
- Dutta, P., Mishra, A., Khandelwal, S., & Katthawala, I. (2020). A multiobjective optimization model for sustainable reverse logistics in Indian E-commerce market. *Journal of Cleaner Production*, 249, 119348.
- Fahimnia, B., Jabbarzadeh, A., Ghavamifar, A., & Bell, M. (2017). Supply chain design for efficient and effective blood supply in disasters. *International Journal of Production Economics*, 183, 700–709.
- Fathollahi-Fard, A. M., Hajiaghahi-Keshтели, M., & Mirjalili, S. (2018). Multi-objective stochastic closed-loop supply chain network design with social considerations. *Applied Soft Computing*, 71, 505–525.
- Fathollahi-Fard, A. M., Dulebenets, M. A., Hajiaghahi-Keshтели, M., Tavakkoli-Moghaddam, R., Safaeian, M., & Mirzahasseinian, H. (2021). Two hybrid meta-heuristic algorithms for a dual-channel closed-loop supply chain network design problem in the tire industry under uncertainty. *Advanced Engineering Informatics*, 50, 101418.
- Fung, Y. N., Choi, T. M., & Liu, R. (2020). Sustainable planning strategies in supply chain systems: Proposal and applications with a real case study in fashion. *Production Planning and Control*, 31(11–12), 883–902.
- Ghahremani-Nahr, J., Kian, R., & Sabet, E. (2019). A robust fuzzy mathematical programming model for the closed-loop supply chain network design and a whale optimization solution algorithm. *Expert Systems with Applications*, 116, 454–471.
- Ghelichi, Z., Saïdi-Mehrabad, M., & Pishvae, M. S. (2018). A stochastic programming approach toward optimal design and planning of an integrated green biodiesel supply chain network under uncertainty: A case study. *Energy*, 156, 661–687.
- Golpîra, H., Najafi, E., Zandieh, M., & Sadi-Nezhad, S. (2017). Robust bi-level optimization for green opportunistic supply chain network design problem against uncertainty and environmental risk. *Computers and Industrial Engineering*, 107, 301–312.
- González, M. E., Quesada, G., Urrutia, I., & Gavidia, J. V. (2006). Conceptual design of an e-health strategy for the Spanish health care system. *International Journal of Health Care Quality Assurance*, 19(2), 146–157.
- Goodarzian, F., Wamba, S. F., Mathiyazhagan, K., & Taghipour, A. (2021). A new bi-objective green medicine supply chain network design under fuzzy environment: Hybrid metaheuristic algorithms. *Computers and Industrial Engineering*, 160, 107535.
- Govindan, K., Paam, P., & Abtahi, A. R. (2016). A fuzzy multi-objective optimization model for sustainable reverse logistics network design. *Ecological Indicators*, 67, 753–768.
- Govindan, K., Mina, H., & Alavi, B. (2020). A decision support system for demand management in health-care supply chains considering the epidemic outbreaks: A case study of coronavirus disease 2019 (COVID-19). *Transportation Research Part e: Logistics and Transportation Review*, 138, 101967.
- Gündoğdu, F. K., & Kahraman, C. (2020). A novel spherical fuzzy QFD method and its application to the linear delta robot technology development. *Engineering Applications of Artificial Intelligence*, 87, 103348.
- Guo, C., Liu, X., Jin, M., & Lv, Z. (2016). The research on optimization of auto supply chain network robust model under macroeconomic fluctuations. *Chaos, Solitons and Fractals*, 89, 105–114.
- Gupta, A. K., & Nadarajah, S. (2004). *Handbook of beta distribution and its applications*. CRC Press.
- Haktanir, E., & Kahraman, C. (2019). A novel interval-valued Pythagorean fuzzy QFD method and its application to solar photovoltaic technology development. *Computers and Industrial Engineering*, 132, 361–372.
- Hamdan, B., & Diabat, A. (2019). A two-stage multi-echelon stochastic blood supply chain problem. *Computers and Operations Research*, 101, 130–143.
- Hamdan, B., & Diabat, A. (2020). Robust design of blood supply chains under risk of disruptions using Lagrangian relaxation. *Transportation Research Part e: Logistics and Transportation Review*, 134, 101764.
- Han, C. H., Kim, J. K., Choi, S. H., & Kim, S. H. (1998). Determination of information system development priority using quality function development. *Computers and Industrial Engineering*, 35(1–2), 241–244.
- Hasani, A., Mokhtari, H., & Fattahi, M. (2021). A multi-objective optimization approach for green and resilient supply chain network design: A real-life case study. *Journal of Cleaner Production*, 278, 123199.

- Heydari, J., Zaabi-Ahmadi, P., & Choi, T. M. (2018). Coordinating supply chains with stochastic demand by crashing lead times. *Computers and Operations Research*, 100, 394–403.
- Hosseini-Motlagh, S. M., Nouri-Harzvili, M., Choi, T. M., & Ebrahimi, S. (2019). Reverse supply chain systems optimization with dual channel and demand disruptions: Sustainability, CSR investment and pricing coordination. *Information Sciences*, 503, 606–634.
- Ivanov, D. (2020). Predicting the impacts of epidemic outbreaks on global supply chains: A simulation-based analysis on the coronavirus outbreak (COVID-19/SARS-CoV-2) case. *Transportation Research Part e: Logistics and Transportation Review*, 136, 101922.
- Iyengar, K. P., Vaishya, R., Bahl, S., & Vaish, A. (2020). Impact of the coronavirus pandemic on the supply chain in healthcare. *British Journal of Healthcare Management*, 26(6), 1–4.
- Jahangoshai Rezaee, M., Yousefi, S., & Hayati, J. (2017). A multi-objective model for closed-loop supply chain optimization and efficient supplier selection in a competitive environment considering quantity discount policy. *Journal of Industrial Engineering International*, 13(2), 199–213.
- Jeihoonian, M., Zanjani, M. K., & Gendreau, M. (2017). Closed-loop supply chain network design under uncertain quality status: Case of durable products. *International Journal of Production Economics*, 183, 470–486.
- Johnson, D. (1997). The triangular distribution as a proxy for the beta distribution in risk analysis. *Journal of the Royal Statistical Society: Series D (The Statistician)*, 46(3), 387–398.
- Karsak, E. E., Sozer, S., & Alptekin, S. E. (2003). Product planning in quality function deployment using a combined analytic network process and goal programming approach. *Computers and Industrial Engineering*, 44(1), 171–190.
- Keyvanshokoh, E., Ryan, S. M., & Kabir, E. (2016). Hybrid robust and stochastic optimization for closed-loop supply chain network design using accelerated Benders decomposition. *European Journal of Operational Research*, 249(1), 76–92.
- Kim, J., Do Chung, B., Kang, Y., & Jeong, B. (2018). Robust optimization model for closed-loop supply chain planning under reverse logistics flow and demand uncertainty. *Journal of Cleaner Production*, 196, 1314–1328.
- Lee, A. H., Kang, H. Y., Yang, C. Y., & Lin, C. Y. (2010). An evaluation framework for product planning using FANP, QFD and multi-choice goal programming. *International Journal of Production Research*, 48(13), 3977–3997.
- Lima, C., Relvas, S., & Barbosa-Póvoa, A. (2018). Stochastic programming approach for the optimal tactical planning of the downstream oil supply chain. *Computers & Chemical Engineering*, 108, 314–336.
- Lin, Q., Zhao, Q., & Lev, B. (2020). Cold chain transportation decision in the vaccine supply chain. *European Journal of Operational Research*, 283(1), 182–195.
- Liu, Y., Ma, L., & Liu, Y. (2021). A novel robust fuzzy mean-UPM model for green closed-loop supply chain network design under distribution ambiguity. *Applied Mathematical Modelling*, 92, 99–135.
- Lo, S. M., Shen, H. P., & Chen, J. C. (2017). An integrated approach to project management using the Kano model and QFD: An empirical case study. *Total Quality Management and Business Excellence*, 28(13–14), 1584–1608.
- Mardan, E., Govindan, K., Mina, H., & Gholami-Zanjani, S. M. (2019). An accelerated benders decomposition algorithm for a bi-objective green closed loop supply chain network design problem. *Journal of Cleaner Production*, 235, 1499–1514.
- Mirzapour Al-E-Hashem, S. M. J., Malekly, H., & Aryanezhad, M. B. (2011). A multi-objective robust optimization model for multi-product multi-site aggregate production planning in a supply chain under uncertainty. *International Journal of Production Economics*, 134(1), 28–42.
- Mousazadeh, M., Torabi, S. A., & Zahiri, B. (2015). A robust possibilistic programming approach for pharmaceutical supply chain network design. *Computers & Chemical Engineering*, 82, 115–128.
- Nayak, S., & Ojha, A. K. (2019). Solution approach to multi-objective linear fractional programming problem using parametric functions. *Opsearch*, 56(1), 174–190.
- Nur, F., Aboytes-Ojeda, M., Castillo-Villar, K. K., & Marufuzzaman, M. (2021). A two-stage stochastic programming model for biofuel supply chain network design with biomass quality implications. *IIE Transactions*, 53(8), 845–868.
- Nurjanni, K. P., Carvalho, M. S., & Costa, L. (2017). Green supply chain design: A mathematical modeling approach based on a multi-objective optimization model. *International Journal of Production Economics*, 183, 421–432.
- Olivares-Aguila, J., & ElMaraghy, W. (2021). System dynamics modelling for supply chain disruptions. *International Journal of Production Research*, 59(6), 1757–1775.

- Pakdil, F., & Kurtulmuşoğlu, F. B. (2014). Improving service quality in highway passenger transportation: A case study using quality function deployment. *European Journal of Transport and Infrastructure Research*, 14(4), 375–393.
- Peidro, D., Mula, J., Poler, R., & Verdegay, J. L. (2009). Fuzzy optimization for supply chain planning under supply, demand and process uncertainties. *Fuzzy Sets and Systems*, 160(18), 2640–2657.
- Pishvae, M. S., & Khalaf, M. F. (2016). Novel robust fuzzy mathematical programming methods. *Applied Mathematical Modelling*, 40(1), 407–418.
- Pishvae, M. S., Rabbani, M., & Torabi, S. A. (2011). A robust optimization approach to closed-loop supply chain network design under uncertainty. *Applied Mathematical Modelling*, 35(2), 637–649.
- Poudel, S. R., Quddus, M. A., Marufuzzaman, M., & Bian, L. (2019). Managing congestion in a multi-modal transportation network under biomass supply uncertainty. *Annals of Operations Research*, 273(1–2), 739–781.
- Prakash, S., Kumar, S., Soni, G., Jain, V., & Rathore, A. P. S. (2020). Closed-loop supply chain network design and modelling under risks and demand uncertainty: An integrated robust optimization approach. *Annals of Operations Research*, 290(1), 837–864.
- Quddus, M. A., Chowdhury, S., Marufuzzaman, M., Yu, F., & Bian, L. (2018). A two-stage chance-constrained stochastic programming model for a bio-fuel supply chain network. *International Journal of Production Economics*, 195, 27–44.
- Rabbani, M., Momen, S., Akbarian-Saravi, N., Farrokhi-Asl, H., & Ghelichi, Z. (2020). Optimal design for sustainable bioethanol supply chain considering the bioethanol production strategies: A case study. *Computers & Chemical Engineering*, 134, 106720.
- Rohmer, S. U. K., Gerdessen, J. C., & Claassen, G. D. H. (2019). Sustainable supply chain design in the food system with dietary considerations: A multi-objective analysis. *European Journal of Operational Research*, 273(3), 1149–1164.
- Roni, M. S., Eksioğlu, S. D., Cafferty, K. G., & Jacobson, J. J. (2017). A multi-objective, hub-and-spoke model to design and manage biofuel supply chains. *Annals of Operations Research*, 249(1–2), 351–380.
- Shahedi, A., Nasiri, M. M., Sangari, M. S., Werner, F., & Jolai, F. (2022). A stochastic multi-objective model for a sustainable closed-loop supply chain network design in the automotive industry. *Process Integration and Optimization for Sustainability*, 6(1), 189–209.
- Sherafati, M., & Bashiri, M. (2016). Closed loop supply chain network design with fuzzy tactical decisions. *Journal of Industrial Engineering International*, 12(3), 255–269.
- Shin, J., Shin, W. S., & Lee, C. (2013). An energy security management model using quality function deployment and system dynamics. *Energy Policy*, 54, 72–86.
- Sinha, P., Kumar, S., & Prakash, S. (2020). Measuring and mitigating the effects of cost disturbance propagation in multi-echelon apparel supply chains. *European Journal of Operational Research*, 282(1), 148–160.
- Soleimani, H., Seyyed-Esfahani, M., & Shirazi, M. A. (2016). A new multi-criteria scenario-based solution approach for stochastic forward/reverse supply chain network design. *Annals of Operations Research*, 242(2), 399–421.
- Soleimani, H., Govindan, K., Saghafi, H., & Jafari, H. (2017). Fuzzy multi-objective sustainable and green closed-loop supply chain network design. *Computers and Industrial Engineering*, 109, 191–203.
- Sousa-Zomer, T. T., & Miguel, P. A. C. (2017). A QFD-based approach to support sustainable product-service systems conceptual design. *The International Journal of Advanced Manufacturing Technology*, 88(1–4), 701–717.
- Subulan, K., Baykasoğlu, A., Özsoydan, F. B., Taşan, A. S., & Selim, H. (2015). A case-oriented approach to a lead/acid battery closed-loop supply chain network design under risk and uncertainty. *Journal of Manufacturing Systems*, 37, 340–361.
- Talaei, M., Moghaddam, B. F., Pishvae, M. S., Bozorgi-Amiri, A., & Gholamnejad, S. (2016). A robust fuzzy optimization model for carbon-efficient closed-loop supply chain network design problem: A numerical illustration in electronics industry. *Journal of Cleaner Production*, 113, 662–673.
- Tirkolaee, E. B., Mardani, A., Dashtian, Z., Soltani, M., & Weber, G. W. (2020). A novel hybrid method using fuzzy decision making and multi-objective programming for sustainable-reliable supplier selection in two-echelon supply chain design. *Journal of Cleaner Production*, 250, 119517.
- Tosarkani, B. M., & Amin, S. H. (2018a). A possibilistic solution to configure a battery closed-loop supply chain: Multi-objective approach. *Expert Systems with Applications*, 92, 12–26.
- Tosarkani, B. M., & Amin, S. H. (2018b). A multi-objective model to configure an electronic reverse logistics network and third party selection. *Journal of Cleaner Production*, 198, 662–682.

- Tosarkani, B. M., & Amin, S. H. (2019). An environmental optimization model to configure a hybrid forward and reverse supply chain network under uncertainty. *Computers and Chemical Engineering*, *121*, 540–555.
- Tosarkani, B. M., Amin, S. H., & Zolfagharinia, H. (2020). A scenario-based robust possibilistic model for a multi-objective electronic reverse logistics network. *International Journal of Production Economics*, *224*, 107557.
- Tsai, F. M., Bui, T. D., Tseng, M. L., & Wu, K. J. (2020). A causal municipal solid waste management model for sustainable cities in Vietnam under uncertainty: A comparison. *Resources, Conservation and Recycling*, *154*, 104599.
- Tsao, Y. C., Thanh, V. V., Lu, J. C., & Yu, V. (2018). Designing sustainable supply chain networks under uncertain environments: Fuzzy multi-objective programming. *Journal of Cleaner Production*, *174*, 1550–1565.
- Vafaeezhad, T., Tavakkoli-Moghaddam, R., & Cheikhrouhou, N. (2019). Multi-objective mathematical modeling for sustainable supply chain management in the paper industry. *Computers and Industrial Engineering*, *135*, 1092–1102.
- Vahdani, B., & Mohammadi, M. (2015). A bi-objective interval-stochastic robust optimization model for designing closed loop supply chain network with multi-priority queuing system. *International Journal of Production Economics*, *170*, 67–87.
- Van Engeland, J., Beliën, J., De Boeck, L., & De Jaeger, S. (2020). Literature review: Strategic network optimization models in waste reverse supply chains. *Omega*, *91*, 102012.
- Wadhwa, V., & Ravindran, A. R. (2007). Vendor selection in outsourcing. *Computers and Operations Research*, *34*(12), 3725–3737.
- Wang, C. H. (2015). Using quality function deployment to conduct vendor assessment and supplier recommendation for business-intelligence systems. *Computers and Industrial Engineering*, *84*, 24–31.
- Wang, X., Wang, L., Xu, X., & Ji, P. (2014). Identifying employee turnover risks using modified quality function deployment. *Systems Research and Behavioral Science*, *31*(3), 398–404.
- Wieland, U., Fischer, M., Pfitzner, M., & Hilbert, A. (2015). Process performance measurement system—towards a customer-oriented solution. *Business Process Management Journal*, *21*(2), 312–331.
- Yavari, M., & Geraeli, M. (2019). Heuristic method for robust optimization model for green closed-loop supply chain network design of perishable goods. *Journal of Cleaner Production*, *226*, 282–305.
- Yousefi, S., & Tosarkani, B. M. (2022). An analytical approach for evaluating the impact of blockchain technology on sustainable supply chain performance. *International Journal of Production Economics*, *246*, 108429.
- Yousefi, S., Jahangoshai Rezaee, M., & Solimanpur, M. (2021). Supplier selection and order allocation using two-stage hybrid supply chain model and game-based order price. *Operational Research*, *21*(1), 553–588.
- Yu, H., & Solvang, W. D. (2018). Incorporating flexible capacity in the planning of a multi-product multi-echelon sustainable reverse logistics network under uncertainty. *Journal of Cleaner Production*, *198*, 285–303.
- Yu, J., Gan, M., Ni, S., & Chen, D. (2018). Multi-objective models and real case study for dual-channel FAP supply chain network design with fuzzy information. *Journal of Intelligent Manufacturing*, *29*(2), 389–403.
- Zahiri, B., Torabi, S. A., Mohammadi, M., & Aghabegloo, M. (2018). A multi-stage stochastic programming approach for blood supply chain planning. *Computers & Industrial Engineering*, *122*, 1–14.
- Zaim, S., Sevklı, M., Camgöz-Akdağ, H., Demirel, O. F., Yayla, A. Y., & Delen, D. (2014). Use of ANP weighted crisp and fuzzy QFD for product development. *Expert Systems with Applications*, *41*(9), 4464–4474.
- Zandkarimkhani, S., Mina, H., Biuki, M., & Govindan, K. (2020). A chance constrained fuzzy goal programming approach for perishable pharmaceutical supply chain network design. *Annals of Operations Research*, *295*, 425–452.
- Zarei, J., Amin-Naseri, M. R., Khorasani, A. H. F., & Kashan, A. H. (2020). A sustainable multi-objective framework for designing and planning supply chain of natural gas components. *Journal of Cleaner Production*, *259*, 120649.
- Zhang, S., Lee, C. K. M., Wu, K., & Choy, K. L. (2016). Multi-objective optimization for sustainable supply chain network design considering multiple distribution channels. *Expert Systems with Applications*, *65*, 87–99.
- Zhang, J., Choi, T. M., & Cheng, T. C. E. (2020). Stochastic production capacity: A bane or a boon for quick response supply chains? *Naval Research Logistics (NRL)*, *67*(2), 126–146.
- Zokaei, S., Jabbarzadeh, A., Fahimnia, B., & Sadjadi, S. J. (2017). Robust supply chain network design: An optimization model with real world application. *Annals of Operations Research*, *257*(1–2), 15–44.

Publisher's Note Springer Nature remains neutral with regard to jurisdictional claims in published maps and institutional affiliations.

Springer Nature or its licensor holds exclusive rights to this article under a publishing agreement with the author(s) or other rightsholder(s); author self-archiving of the accepted manuscript version of this article is solely governed by the terms of such publishing agreement and applicable law.